Direct binding of TUBB3 with DCC couples netrin-1 signaling to intracellular microtubule dynamics in axon outgrowth and guidance

Chao Qu, Trisha Dwyer, Qiangqiang Shao, Tao Yang, Huai Huang and Guofa Liu*

Department of Biological Sciences, University of Toledo, M.S. 601, 2801 W. Bancroft Street, Toledo, OH 43606, USA

*Author for correspondence (Guofa.Liu@utoledo.edu)

Accepted 5 April 2013
Journal of Cell Science 126, 3070–3081

doi: 10.1242/jcs.122184

Summary

The coupling of axon guidance cues, such as netrin-1, to microtubule (MT) dynamics is essential for growth cone navigation in the developing nervous system. However, whether axon guidance signaling regulates MT dynamics directly or indirectly is unclear. Here, we report that TUBB3, the most dynamic β-tubulin isoform in neurons, directly interacts with the netrin receptor DCC, and that netrin-1 induces this interaction in primary neurons. TUBB3 colocalizes with DCC in the growth cones of primary neurons and MT dynamics is required for netrin-1-promoted association of TUBB3 with DCC. Netrin-1 not only increases co-sedimentation of DCC with polymerized MT, but also promotes MT dynamics in the growth cone. Knocking down TUBB3 inhibits netrin-1-induced MT dynamics, axon outgrowth and attraction *in vitro* and causes defects in commissural axon projection in the embryo. These results indicate that TUBB3 directly links netrin signaling pathways to MT dynamics and plays an important role in guiding commissural axons *in vivo*.

Key words: DCC, Signal transduction, TUBB3, Axon guidance, Microtubule dynamics, Netrin

Introduction

In the nervous system, temporal and spatial information processing relies on a variety of functional neural circuitries. The formation of neural circuits during brain development depends on the precise coordination of different guidance cues, their receptors and intracellular signal transduction cascades (Dent et al., 2011; Guan and Rao, 2003; Kolodkin and Tessier-Lavigne, 2011), which eventually converges on orchestrating the cytoskeleton dynamics to maneuver growth cone navigation (Kalil and Dent, 2005; Lowery and Van Vactor, 2009; Vitriol and Zheng, 2012). The coordination of actin filament and microtubule (MT) dynamics in neurons plays a crucial role in axon pathfinding in the developing nervous system (Buck and Zheng, 2002; Dent and Gertler, 2003; Dent et al., 2011; Lowery and Van Vactor, 2009; Vitriol and Zheng, 2012). However, whether MT dynamics are directly regulated by guidance cues and how intracellular signaling initiated by the activation of guidance receptors modulates MT dynamics are still unclear.

Netrins, a family of canonical guidance cues, is a typical model for studying molecular mechanisms of axon outgrowth and guidance in the developing nervous system (Hedgecock et al., 1990; Ishii et al., 1992; Kennedy et al., 1994; Kolodziej et al., 1996; Tessier-Lavigne et al., 1988). As bifunctional guidance cues, netrins act as either chemoattractants or chemorepellents for different cell types (Alcántara et al., 2000; Colamarino and Tessier-Lavigne, 1995). The mammalian receptors of netrins are Deleted in Colorectal Cancer (DCC) (Fazeli et al., 1997; Keino-Masu et al., 1996), neogenin (Keeling et al., 1997; Keino-Masu et al., 1996), Uncoordinated-5 (UNC5) (Ackerman et al., 1997; Leonardo et al., 1997), and Down Syndrome Cell Adhesion Molecule (DSCAM) (Liu et al., 2009; Ly et al., 2008). The phenotypic defects in DCC-deficient mouse embryos are similar to those in netrin-1$^{-/-}$ mice embryos with aberrant commissural axon pathfinding and, ultimately, the inability of most commissural axons to reach the floor plate and cross the midline (Fazeli et al., 1997; Serafini et al., 1994). DCC collaborates with DSCAM mediating netrin-1-induced axon outgrowth and chemoattraction (Liu et al., 2009; Ly et al., 2008), whereas interaction of UNC-5 with DCC or DSCAM mediates repulsion (Finger et al., 2002; Hong et al., 1999; Keino-Masu et al., 1996; Kolodziej et al., 1996; Leonardo et al., 1997; Purohit et al., 2012), indicating the coordination of different netrin receptors is crucial for their ability to mediate attraction or repulsion.

Recent studies have shown that mutations in *TUBB3*, a neuronal β-tubulin isotype III, result in commissural axon malformation both in human patients and mouse models with dysgenesis of the corpus callosum, anterior commissure, and internal capsule, suggesting TUBB3 is required for axon guidance and neuronal development (Poirier et al., 2010; Tischfield et al., 2010). Here, we have found that DCC interacts directly with TUBB3, and netrin-1 induces this interaction depending on MT dynamics in primary neurons. TUBB3 is required for netrin-induced axon outgrowth and pathfinding in the developing nervous system. These results demonstrate, to our knowledge for the first time, that guidance receptors directly couple MT dynamics in axon guidance.

Results

TUBB3 interacts with the netrin receptor DCC

To examine the potential interaction of TUBB3 with DCC in the developing brain, primary neurons from the cerebral cortex of

embryonic day 15 (E15) mice were isolated, cultured and treated with conditioned media from control HEK cells or HEK cells stably expressing human netrin-1. The cell extracts were immunoprecipitated with anti-DCC antibody before probing the blots with the anti-TUBB3 antibody. Anti-DCC antibody immunoprecipitated TUBB3 (Fig. 1A). In contrast, as predicted, TUBB3 was not present when primary antibody was omitted (see the 'IgG' control lanes in Fig. 1A). Treatment with netrin-1 conditioned media increased the interaction of TUBB3 with DCC (Fig. 1A; quantification in Fig. 1C, upper panel). Netrins play a crucial role in promoting commissural neuron axon outgrowth and pathfinding in the developing spinal cord (Kennedy et al., 1994; Serafini et al., 1994). To determine whether endogenous TUBB3 interacted with DCC in spinal cord neurons, dissociated cells from the dorsal half of E13 mouse spinal cords were cultured and treated with netrin-1 conditioned media. The immunoprecipitation results indicated that DCC interacted with TUBB3 and netrin-1 dramatically increased this interaction (Fig. 1B; quantification in Fig. 1C, lower panel). Netrin-1 increased the interaction of TUBB3 with DCC within 5 minutes and the induction lasted up to 20 minutes after netrin-1 stimulation (Fig. 1D). Similar time-courses of netrin-1 stimulation were observed in E15 cortical neurons (data not shown). To confirm that netrin-1 was directly responsible for increasing the interaction of TUBB3 with DCC, we tested purified netrin-1 from two sources: chicken netrin-1 from a commercial source and human netrin-1 purified from a stable HEK cell line established in our lab. Both sources of netrin-1 increased the interaction of TUBB3 with DCC in E15 primary cortical neurons in a dose-dependent manner (Fig. 1E). In contrast, DCC could not interact with TUBB1 and TUBB2, two other β-tubulin subunits, in the absence or presence of purified netrin-1 (Fig. 1F). These results strongly suggest that TUBB3 specifically associates with DCC in primary neurons.

To determine whether TUBB3 could interact directly with DCC, cDNAs expressing HA-tagged human TUBB3 were co-transfected with DCC-Myc into HEK293 cells that do not share the same signaling machinery with primary neurons. Anti-HA antibody immunoprecipitated DCC (Fig. 1G), detected by probing the blots with anti-Myc antibody. This result suggests that TUBB3 may directly interact with DCC. To further characterize this direct interaction, the isolated intracellular domain of DCC (DCC-ICD-MBP) was purified and incubated with purified TUBB3. TUBB3 appeared to interact directly with the intracellular domains of DCC (Fig. 1H). DCC has three conserved intracellular domains (P1, P2, P3) that are required for netrin-mediated signal transduction. To identify the DCC domain(s) that interact with TUBB3, TUBB3 was cotransfected

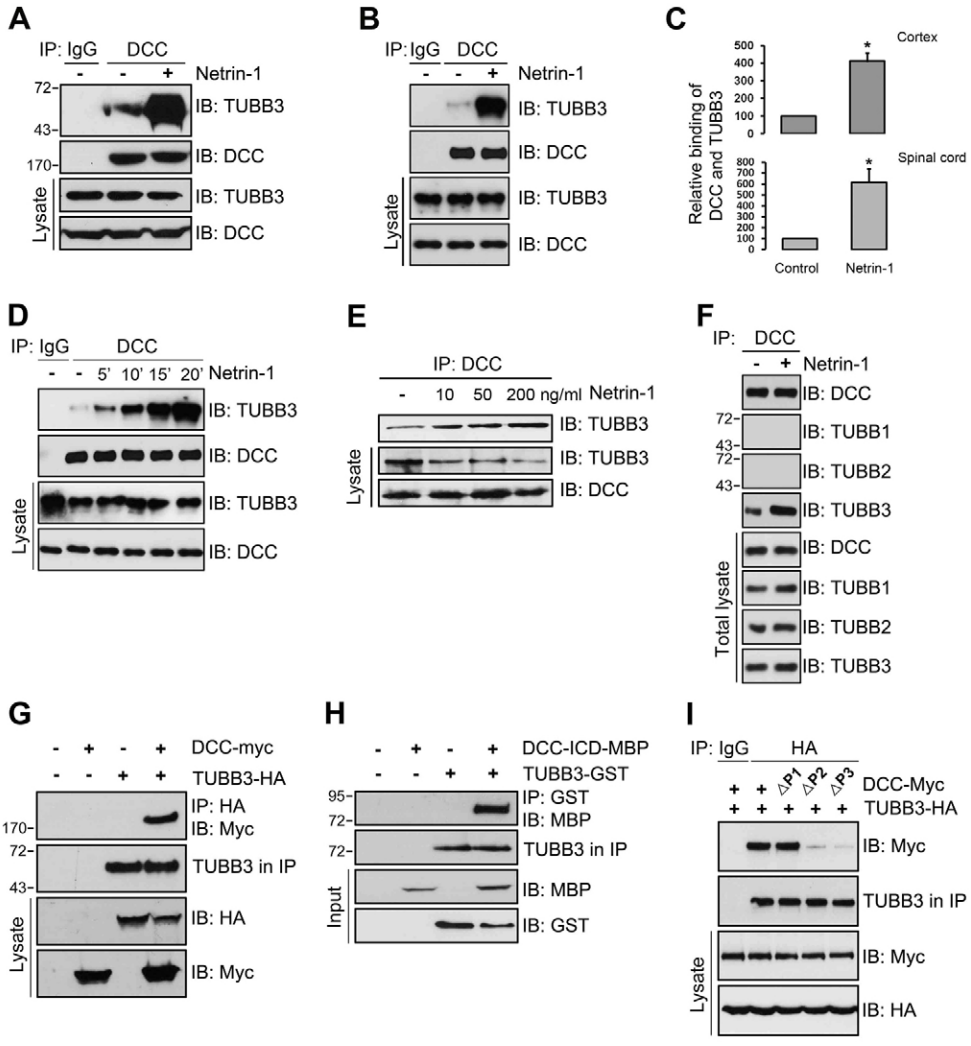

Fig. 1. Interaction of TUBB3 with DCC. (**A**,**B**) Interaction of endogenous TUBB3 with DCC in E15 cortical (A) and E13 dorsal spinal cord (B) neurons. (**C**) Quantification of A and B from three independent experiments; $*P<0.05$ (two-tailed Student's *t*-test). (**D**) Netrin-1 increased the interaction of endogenous TUBB3 with DCC in a time-dependent manner. Lysates of dissociated neurons from E13 mouse spinal cords were immunoprecipitated with anti-DCC and analyzed with anti-TUBB3. (**E**) Netrin-1 increased the interaction of endogenous TUBB3 with DCC in a dose-dependent manner. E15 primary cortical neurons were treated with purified netrin-1 at 10, 50 and 200 ng/ml. (**F**) Endogenous DCC interacted with TUBB3, not TUBB1 and TUBB2, in E15 cortical neurons with or without netrin-1 treatment. Cell lysates of dissociated neurons from E15 mouse cortexes were immunoprecipitated with anti-DCC and followed by probing with anti-TUBB1, anti-TUBB2 or anti-TUBB3. (**G**) Interaction of TUBB3 with DCC in HEK293 cells. TUBB3-HA was co-transfected with DCC-Myc into HEK293 cells. Anti-HA (TUBB3) precipitated DCC-Myc. (**H**) Direct interaction of TUBB3 with DCC. Purified TUBB3 was incubated with purified intracellular domain of DCC tagged with MBP *in vitro*. The anti-GST antibody was used to immunoprecipitate proteins and the blot was analyzed with anti-MBP. (**I**) P2 and P3 domains in DCC are required for the interaction of DCC and TUBB3. TUBB3-HA was co-transfected with different truncated DCCs (DCC-ΔP1, ΔP2 and ΔP3) tagged with Myc in HEK293 cells.

with three distinct DCC truncation mutants, ΔP1 (deletion of residues 1147–1171) or ΔP2 (deletion of residues 1335–1356) or ΔP3 (deletion of residues 1426–1447) into HEK293 cells. TUBB3 bound to a truncated DCC lacking the P1 domain, but did not bind to truncated DCCs lacking either the P2 or P3 domains (Fig. 1I). These results suggest that the intracellular P2 and P3 domains of DCC may be required for its interaction with TUBB3.

Axon growth cones are highly motile sensory structures in developing neurons that respond to extracellular guidance cues. To determine whether TUBB3 is subcellularly colocalized with DCC in the growth cone of primary neurons, tissues from the E11 dorsal spinal cord and E15 cortex were dissociated and cultured. The localization of DCC and TUBB3 overlapped in the growth cones of E11 commissural neurons after 4-day culture (supplementary material Fig. S1A–C). DCC colocalized with TUBB3 in the peripheral (P) region of growth cones, including lamellipodia and filopodia (supplementary material Fig. S1A–C). Colocalization of TUBB3 with DCC was also observed in growth cones of E15 cortical neurons (supplementary material Fig. S1D–F).

MT dynamics modulates the interaction of TUBB3 with DCC

The modulation of MT dynamics in growth cones plays a crucial role in axon guidance (Dent et al., 2011). To investigate whether MT dynamics is required for the binding of TUBB3 with DCC, primary E15 cortical neurons were treated with paclitaxel (taxol) or nocodazole, drugs that disrupt MT dynamics. As expected based on the results described above, netrin-1 increased the interaction of endogenous TUBB3 with DCC (Fig. 2A–C). The netrin-1-induced interaction was inhibited by both the MT-stabilizing drug taxol and the MT-destabilizing drug nocodazole (Fig. 2A–C), indicating that MT dynamics is required for the netrin-1 dependent interaction of TUBB3 with DCC. To further determine whether monomeric or polymeric TUBB3 binds to DCC, a MT co-sedimentation assay was performed on E15 cortical neuron cell lysates. Because MT in cell lysates becomes unstable *in vitro* and constantly depolymerizes under cold conditions, incubation of the lysate on ice induced MT depolymerization and yielded monomerized TUBB3 subunits in the soluble supernatant and polymerized TUBB3 in the pellet after centrifugation (Fig. 2D,F). Most of the endogenous DCC also remained in the supernatants with or without netrin-1 stimulation (Fig. 2D,E). In contrast, in the presence of taxol in cell lysate stabilizing MT against depolymerization by cold treatment, DCC co-sedimented with polymerized MT with a large quantity of DCC and TUBB3 in the pellet (Fig. 2D; quantification in Fig. 2E,F). As predicted, in the presence of taxol, netrin-1 further increased DCC and TUBB3 in the pellets (Fig. 2D; quantification in Fig. 2E,F). These results indicate that netrin-1 induces the interaction of endogenous DCC with polymerized TUBB3 in primary neurons, suggesting that the interaction may be dependent on MT dynamics. To determine whether netrin-1 directly modulates MT dynamics, EB3-GFP, a marker of MT dynamics in live cells, was transfected into either E13 dorsal spinal cord neurons (supplementary material Fig. S2; supplementary material Movies 1–4) or E15 cortical neurons (data not shown). Results from live cell imaging revealed that

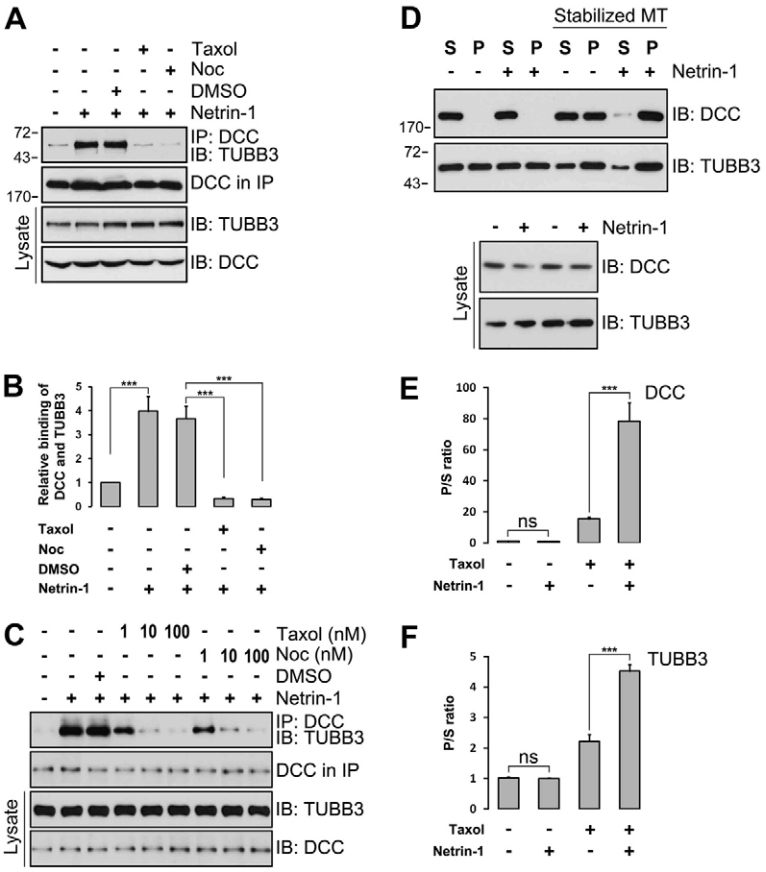

Fig. 2. The induction of the interaction of TUBB3 with DCC by netrin-1 depends on MT dynamics. (**A**–**C**) Taxol and nocodazole (Noc) inhibited netrin-1-induced interactions of endogenous TUBB3 with DCC. E15 cortical neurons were treated with purified netrin-1 in the presence of different concentrations of taxol or nocodazole (1 μM taxol and 3 μM nocodazole in A). (**B**) Quantification of A from three independent experiments showing relative binding of DCC and TUBB3. (**D**–**F**) E15 cortical neurons were stimulated with netrin-1 and the co-sedimentation assay of cell lysates was performed in the absence or presence of taxol. DCC and TUBB3 in the pellet (P) and supernatant (S) fractions were examined by western blot using anti-DCC and anti-TUBB3, respectively. (E,F) Quantification of three independent experiments showing P/S ratio of DCC (E) and TUBB3 (F), respectively. Netrin-1 increased the co-sedimentation of DCC and TUBB3 with polymerized MTs in primary neurons. ns, not significant; ***$P<0.001$ (two-tailed Student's *t*-test).

netrin-1 increased the percentage of moving EB3-GFP comets in the growth cone of primary spinal cord neurons (supplementary material Fig. S2; supplementary material Movies 1 and 2) and cortical neurons (data not shown), and TUBB3 knockdown blocked this induction (supplementary material Fig. S2C; supplementary material Movies 3 and 4, data not shown for cortical neurons). These data suggest that netrin-1 directly modulates MT dynamics via TUBB3.

Tyrosine phosphorylation is required for netrin signaling and the post-translation modification (PTM) of MT subunits is crucial for intracellular MT organization and dynamics. To investigate whether tyrosine phosphorylation of TUBB3 is involved in netrin signaling, primary neurons from E13 spinal cords and E15 cortexes were dissociated and examined for the TUBB3 tyrosine phosphorylation in the presence of or absence of netrin-1 (Fig. 3A–C; supplementary material Fig. S3A,B). Immunoprecipitation experiments demonstrated that the tyrosine phosphorylation of TUBB3 was increased by netrin-1 in a dose- and time-dependent manner (Fig. 3A–C; supplementary material Fig. S3A). Netrin-1-induced TUBB3 tyrosine phosphorylation was inhibited by PP2, an inhibitor of the Src family kinases, but not PP3, an inactive control for PP2 (Fig. 3D; supplementary material Fig. S3B). The netrin-1-dependent induction of the endogenous interaction of TUBB3 with DCC in E15 neurons was also inhibited by PP2 (Fig. 3E,F). These findings indicate that Src family kinases are required for the netrin-1-induced tyrosine phosphorylation of TUBB3 and the interaction of TUBB3 with DCC. To further examine the role of Src family kinases in the netrin-1-induced binding of endogenous DCC to dynamic TUBB3, these key proteins were co-sedimented from lysates of dissociated E15 primary cortical neurons after netrin-1 stimulation (Fig. 3G,H). As expected, netrin-1 increased the amount of DCC in the MT-sedimented pellets (Fig. 3G,H) and PP2, not PP3, inhibited the netrin-1-induced co-sedimentation of DCC and MTs (Fig. 3G,H). These results suggest that Src family kinases play an important role in regulating the dynamic interaction of TUBB3 with DCC in primary neurons.

TUBB3 is required for netrin-1-induced neurite outgrowth

To study the function of TUBB3 in netrin-1 signaling, a TUBB3 siRNA pool (Dharmacon) or short hairpin-based RNA interference constructs (TUBB3 shRNAs, gift from David L. Turner, University of Michigan, targeting a sequence common to mouse and chicken TUBB3) (Yu et al., 2002) were transfected into E15 mouse cortical neurons (Fig. 4K) and chicken neural tubes at stage 12–15 (Fig. 5K). The siRNA pool and one shRNA construct significantly reduced the level of endogenous TUBB3 in these neurons (Fig. 4K; Fig. 5K) and were used in subsequent experiments.

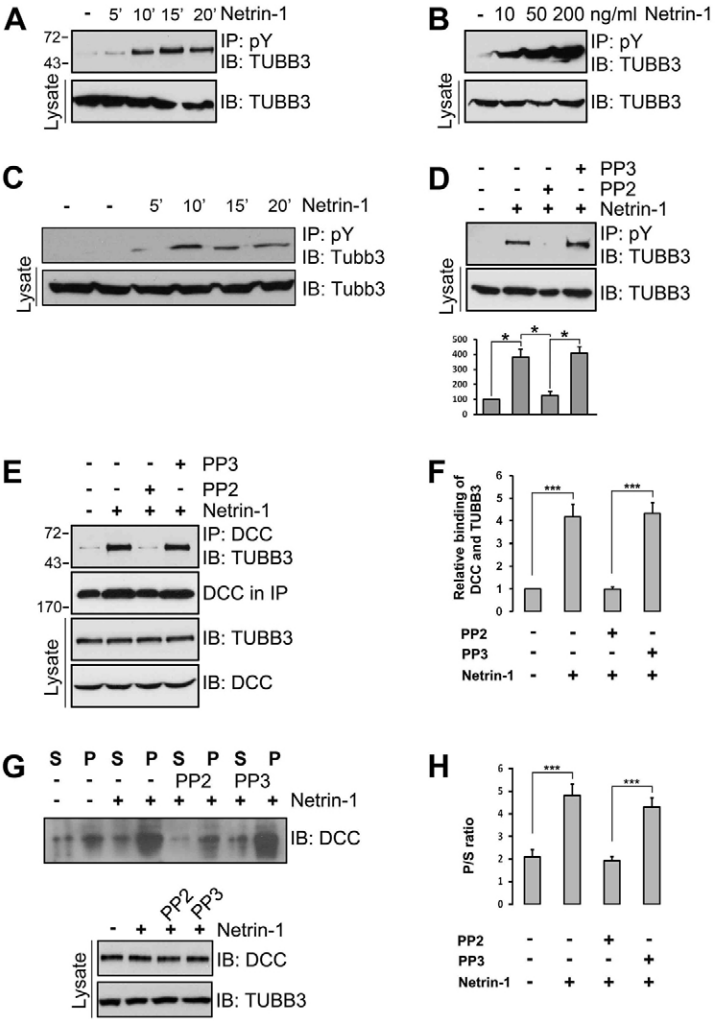

Fig. 3. Src family kinase activity is required for the induction of TUBB3 tyrosine phosphorylation and the interaction of TUBB3 with DCC by netrin-1. (**A**,**B**) Induction of TUBB3 tyrosine phosphorylation in dissociated cortical neurons by netrin-1. E15 cortical neurons were treated with purified netrin-1 for 5–20 minutes. The anti-pY antibody was used to immunoprecipitate proteins and the immunoblot was analyzed with anti-TUBB3. (**C**) Induction of TUBB3 tyrosine phosphorylation in dissociated E13 dorsal spinal cord neurons by netrin-1. Primary neurons were treated with purified netrin-1 (200 ng/ml). (**D**) Src family kinase-specific inhibitor PP2 inhibited netrin-1-induced TUBB3 tyrosine phosphorylation. E15 cortical cells were stimulated with netrin-1 in the presence of PP2 or PP3. Quantification is shown in the lower panel (Student's *t*-test). (**E**) PP2, but not PP3, blocked netrin-1-induced interaction of endogenous TUBB3 with DCC in primary neurons. (**F**) Quantification showing relative binding of DCC and TUBB3 in E. (**G**,**H**) Netrin-1-stimulated co-sedimentation of DCC with MTs was inhibited by PP2, not PP3. E15 cortical neurons were stimulated with netrin-1 in the presence of PP2 or PP3. DCC in the pellet and supernatant fractions was examined by western blot. Quantification of G is shown in H (one-way ANOVA and Fisher LSD post-hoc comparisons). $*P<0.05$, $***P<0.001$.

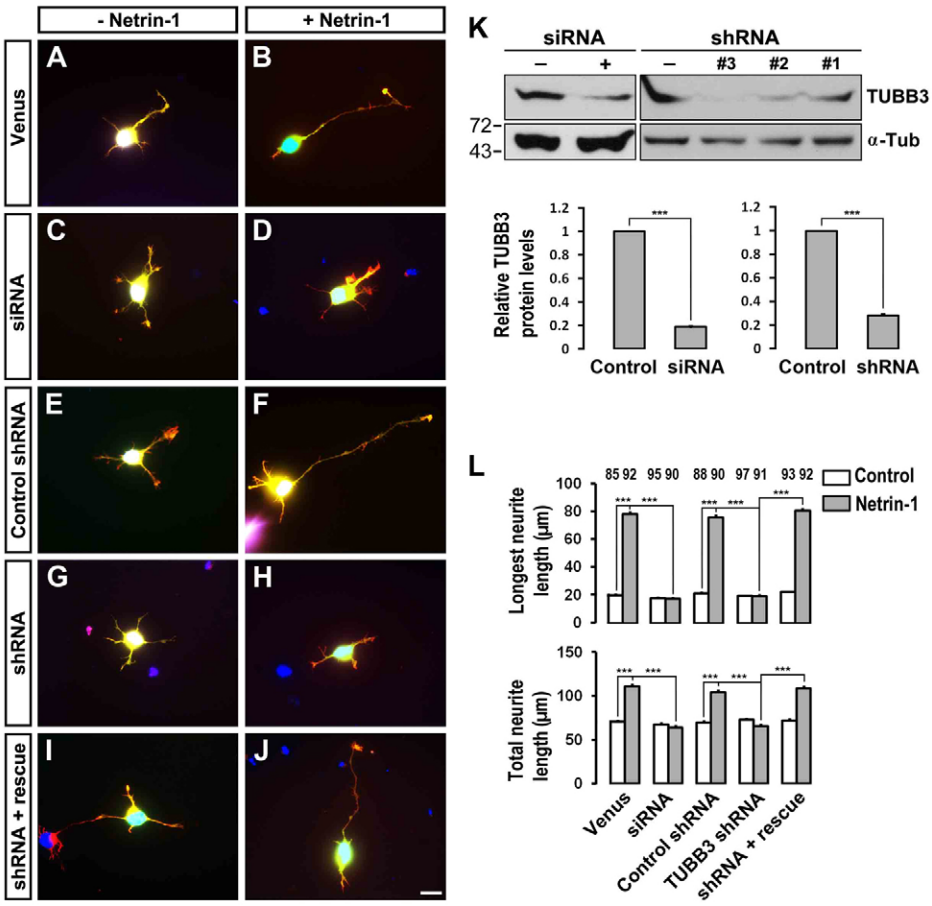

Fig. 4. Inhibition of netrin-1-induced axon outgrowth of cortical neurons by TUBB3 knockdown. (**A**–**J**) E15 mouse cortical neurons were transfected with Venus YFP only (A,B), Venus YFP plus the TUBB3 siRNA pool (C,D), Venus YFP plus control shRNA (E,F), Venus YFP plus TUBB3 shRNA (G,H) and Venus YFP plus shRNA and the wild-type human RNAi-resistant TUBB3 (I,J). Neurite outgrowth from YFP-positive neurons was assessed in the presence of purified netrin-1 (B,D,F,H,J) and in the sham-purified control (A,C,E,G,I). (**K**) Both TUBB3 siRNA pool and shRNA (#3) reduced endogenous TUBB3 protein levels in E15 cortical neurons (Student's *t*-test). (**L**) Quantification of netrin-1-induced neurite outgrowth. Only the neurites of YFP-positive neurons not in contact with other cells were measured and used in the statistical analyses. Data are mean ± s.e.m. from three separate experiments. The numbers on the top of each bar indicate the numbers of neurons tested in the corresponding groups (one-way ANOVA with Fischer LSD for post-hoc comparisons). ***$P<0.001$. Scale bar: 10 μm.

To examine whether TUBB3 is involved in netrin-1-induced neurite outgrowth, primary cortical neurons from E15 mice were dissociated and transfected with a construct expressing Venus yellow fluorescent protein (Venus YFP) only (Fig. 4A,B) or Venus YFP together with the TUBB3 siRNA pool (Fig. 4C,D), the control shRNA (Fig. 4E,F), the TUBB3 shRNA (Fig. 4G,H) or the TUBB3 shRNA plus the RNAi-resistant rescue constructs (Fig. 4I,J), respectively, as we have described previously (Li et al., 2008; Liu et al., 2007; Liu et al., 2009). These neurons were stimulated with netrin-1 and cultured for 20 hours. In neurons transfected with the Venus YFP only, neurite outgrowth was stimulated by netrin-1 (Fig. 4A,B; quantification in Fig. 4L). As predicted, either the TUBB3 siRNA pool (Fig. 4C,D) or TUBB3 shRNA (Fig. 4G,H), but not control TUBB3 shRNA (Fig. 4E,F), inhibited netrin-1-induced neurite outgrowth (quantification in Fig. 4L). Importantly, the expression of the wild-type human RNAi-resistant TUBB3 rescued netrin-1-promoted neurite outgrowth in neurons treated with TUBB3 siRNA (Fig. 4I,J; quantification in Fig. 4L).

To examine the role of TUBB3 in netrin-1-induced commissural axon outgrowth, we examined cultured chick dorsal spinal cord explants, as described previously (Liu et al., 2009). The TUBB3 siRNA pool or shRNA together with Venus YFP plasmids were introduced into chicken neural tubes at stage 12–15, and the YFP-labeled dorsal spinal cord segments were dissected at stage 18–20. Axon outgrowth was quantified by measuring the numbers of axon bundles and the total axon length per explant. In explants transfected with Venus YFP only (Fig. 5A,B) or with Venus YFP plus control shRNA (Fig. 5E,F), netrin-1 significantly induced axon outgrowth (quantification in Fig. 5L,M). TUBB3 siRNA (Fig. 5C,D) or shRNA (Fig. 5G,H), but not control shRNA (Fig. 5E,F), significantly inhibited netrin-1-induced axon outgrowth (quantification in Fig. 5L,M). The expression of wild-type human TUBB3, which is resistant to TUBB3 shRNA, rescued the effect of TUBB3 knockdown on netrin-1-induced axon outgrowth (Fig. 5I,J; quantification in Fig. 5L,M). These results indicate that TUBB3 is required for netrin-1-induced commissural axon outgrowth *in vitro*. Basal axon outgrowth of either dissociated E15 mouse cortical neurons or chick spinal cord commissural neurons was not affected by TUBB3 knockdown (Figs 4 and 5; supplementary material Fig. S4). In addition, TrkB, a receptor of BDNF, could not interact with endogenous TUBB3 in the absence or presence of BDNF (supplementary material Fig. S4A,B) and knockdown of TUBB3 did not affect BDNF-induced axon outgrowth of primary cortical neurons (supplementary material Fig. S4C–I). These data suggest that TUBB3 is specifically involved in netrin-1-induced axon outgrowth. Furthermore, overexpression of DCC intracellular P2–3 domain not only inhibited the interaction of TUBB3 with full-length wild-type DCC in HEK293 cells (supplementary material Fig. S5A,B), but also abolished netrin-1-induced neurite outgrowth of E15 cortical neurons (supplementary material Fig. S5C–G), suggesting that DCC-TUBB3 interaction is required for netrin-1-induced axon outgrowth.

TUBB3 is required for axon attraction by netrin-1

Netrin-1 plays a crucial role in attracting the commissural axon projection in the developing neural tube (Kennedy et al., 1994;

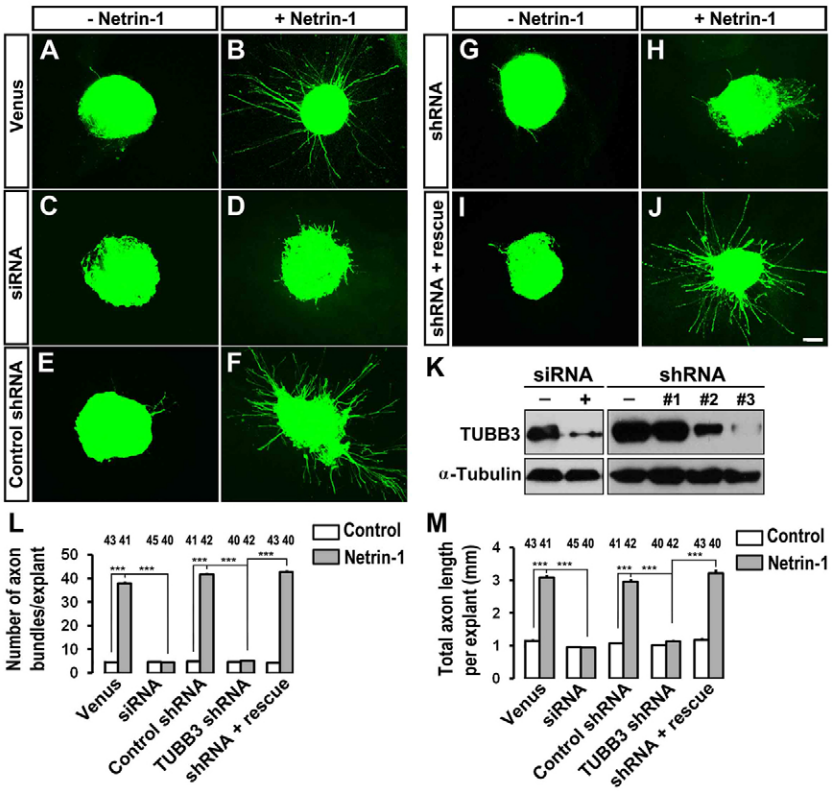

Fig. 5. Inhibition of netrin-1-induced axon outgrowth of chick dorsal spinal cord explants by TUBB3 knockdown. (**A**–**J**) Chick neural tubes were electroporated *in ovo* at stage 12–15 with Venus YFP only (A,B), Venus YFP plus the TUBB3 siRNA pool (C,D), Venus YFP plus control shRNA (E,F), Venus YFP plus TUBB3 shRNA (G,H) and Venus YFP plus TUBB3 shRNA and the wild-type human RNAi-resistant TUBB3 (I,J). Netrin-1 increased commissural axon outgrowth with longer and more axon bundles in the netrin-1 group (B,F) than the control group (A,E). Netrin-1-induced axon outgrowth was inhibited either by the TUBB3 siRNA pool (C,D) or shRNA (G,H). The expression of the wild-type human RNAi-resistant TUBB3 plasmids reversed the effect of TUBB3 shRNA (I,J). (**K**) Both TUBB3 siRNA pool and shRNA efficiently knocked down endogenous TUBB3 in chick spinal cords. (**L**,**M**) Quantification of netrin-1-induced commissural axon outgrowth. Only YFP-positive axon bundles were measured and used in the statistical analyses. The numbers on the top of each bar indicate the numbers of explants tested in the corresponding groups. Data are mean ± s.e.m. from three separate experiments. ***$P<0.001$ (one-way ANOVA with Fischer LSD for post-hoc comparisons). Scale bar: 100 μm.

Serafini et al., 1996; Serafini et al., 1994; Tessier-Lavigne et al., 1988). To determine whether TUBB3 is required for commissural axon turning towards netrin-1, we used the open-book assay with commissural axons from chick embryos as illustrated in Fig. 6A (Li et al., 2008; Liu et al., 2004; Liu et al., 2007; Liu et al., 2009). The Venus YFP construct was electroporated either alone or with the TUBB3 siRNA pool, TUBB3 control shRNA, TUBB3 shRNA, and TUBB3 shRNA plus TUBB3 RNAi-resistant constructs, respectively, into the chick neural tube at stages 12–15. The electroporated neural tube (visualized by green fluorescence) was then isolated and laid out as an ‘open book’ at stage 18–20 (Fig. 6A). A rectangle of neural tube explant containing the floor plate was prepared and co-cultured with an aggregate of control HEK293 cells or HEK293 cells that stably secreted netrin-1 for 40 hours (Fig. 6A).

When the neural tube was electroporated with Venus YFP alone, 87.3±8.2% of commissural axons turned towards netrin-1 secreting cell aggregates (Fig. 6C,C′; quantification in Fig. 6L), whereas only 4.9±0.1% of axons projected towards the control cell aggregates not secreting netrin-1 (Fig. 6B,B′; Fig. 6L). TUBB3 siRNA significantly inhibited commissural axons turning toward netrin-1: the turning percentage was reduced from 87.3±8.2% in the Venus YFP with netrin-1 group to 4.8±0.2% in the TUBB3 siRNA with netrin-1 group (Fig. 6C,C′,E,E′; Fig. 6L). To confirm the role of TUBB3 in netrin-1-induced axon turning, TUBB3 shRNA or the control shRNA were introduced into the neural tube by electroporation. When the control shRNA was electroporated into the neural tube together with Venus YFP, 91.3±7.3% of commissural axons turned towards netrin-1 (Fig. 6F–G′; Fig. 6L). In contrast, the co-transfection of TUBB3 shRNA with Venus YFP significantly inhibited netrin-1-induced attraction with only 7.1±0.3% of axons turning towards netrin-1 (Fig. 6H–I′; Fig. 6L). To further determine the specificity of shRNA knockdown, TUBB3 shRNA was electroporated with plasmids encoding a wild-type human RNAi-resistant TUBB3 into the chick neural tube. The wild-type RNAi-resistant TUBB3 transgene rescued the netrin-1 dependent phenotype with 89.1±9.0% of axons turning towards netrin-1 (Fig. 6J,L). In addition, expression of DCC P2–3 domain also inhibited netrin-1-induced axon turning (supplementary material Fig. S5H,I; quantification in Fig. 6L). Together, these results support the hypothesis that TUBB3 is specifically required for netrin-1-induced commissural axon attraction.

TUBB3 is required for spinal commissural axon projection *in vivo*

The results discussed above have shown that TUBB3 plays an important role in the *in vitro* functions of netrin-1 in neurite outgrowth and axon attraction. To determine the *in vivo* role of TUBB3, the effects of TUBB3 siRNA and TUBB3 shRNA were examined on commissural axon projection in the developing chicken spinal cord (Fig. 7) (Li et al., 2008; Liu et al., 2007; Liu et al., 2009). Venus YFP was introduced by electroporation into the neural tube of stage 12 chick embryos *in ovo* and the embryos were allowed to develop until stages 23 (Fig. 7A). The YFP-labeled lumbosacral segments of the spinal cord were isolated and laid out as an ‘open book’ (Fig. 7A). By stage 23, 81.1±3.3% of the commissural axons expressing Venus YFP alone reached the floor plate (Fig. 7B; quantification in Fig. 7G) (Li et al., 2008; Liu et al., 2007; Liu et al., 2009). In contrast, only 15.5±2.6% of the commissural axons transfected with the TUBB3 siRNA pool reached the floor plate (Fig. 7C,G). Similarly, TUBB3 shRNA also significantly inhibited the projection of commissural axons towards the floor plate, while

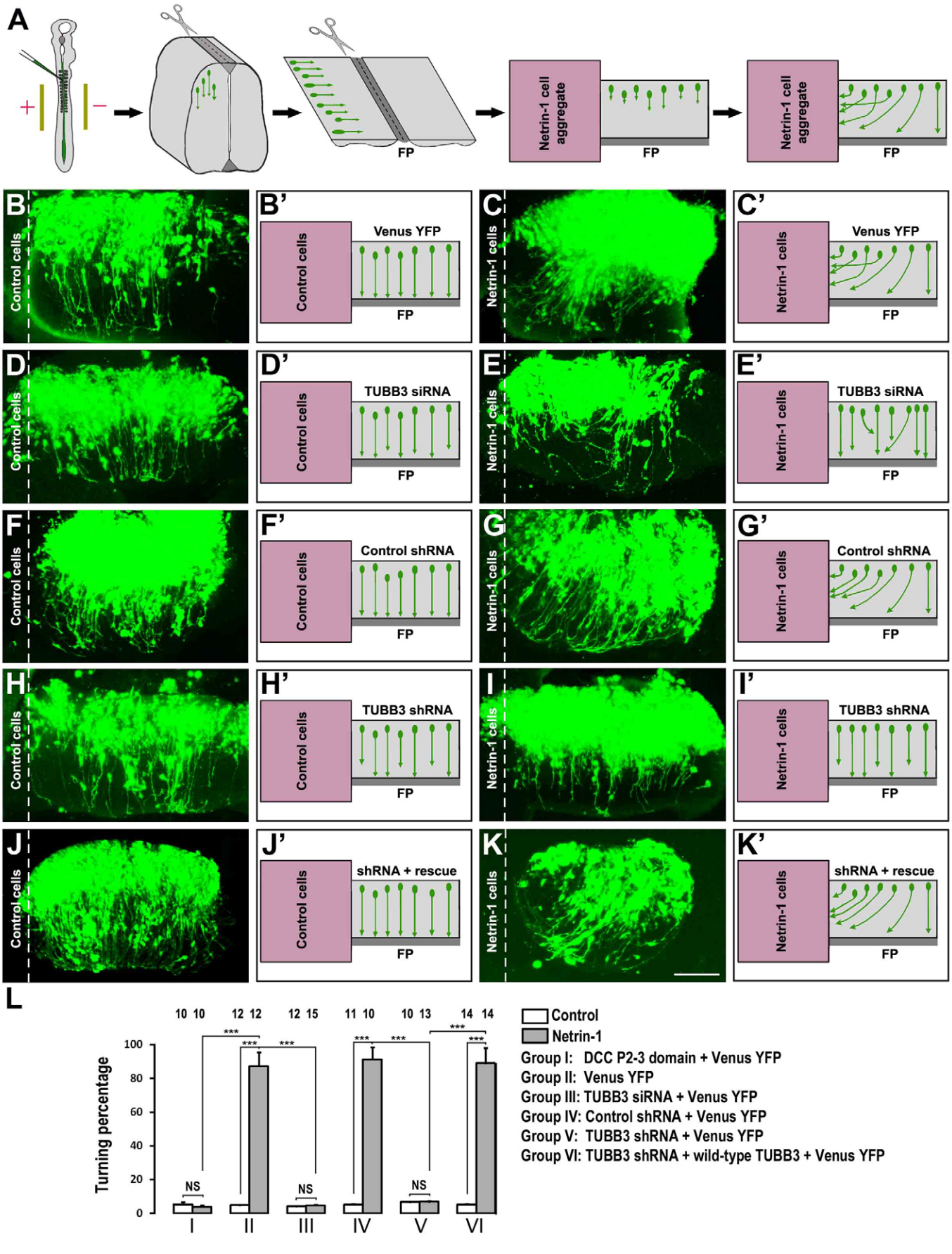

Fig. 6. See next page for legend.

TUBB3 control shRNA had no effect on the projection of commissural axons (Fig. 7D,E,G). The percentage of the YFP-labeled commissural axons per embryo reaching the floor plate was decreased from 79.1±5.3% in the control shRNA group to 24.3±1.3% in the TUBB3 shRNA group. The effect of TUBB3 shRNA on commissural axon projection was reversed by co-transfecting the wild-type RNAi-resistant human TUBB3 plasmid (Fig. 7F,G) with 82.6±4.7% of the YFP-labeled commissural axons per embryo reaching the floor plate.

Although the open-book preparation demonstrated obvious defects in commissural axon projection *in vivo*, it was difficult to effectively assess effects on axon turning. To examine whether knockdown of TUBB3 disrupted commissural axon pathfinding in addition to inhibiting axon extension *in vivo*, either Venus YFP alone or Venus YFP with the TUBB3 siRNA pool were electroporated into chick spinal cord and transverse sections of the chick spinal cord at stage 23 were prepared (Fig. 8A–C). In addition to the inhibition of axon extension, some commissural axons transfected with TUBB3 siRNAs were misguided (Fig. 8C; quantification in Fig. 8G–I) instead of projecting normally towards the floor plate (Fig. 8B; Fig. 8G–I). These phenotypes were further confirmed by expressing Venus YFP and the TUBB3 shRNA in commissural axons that also exhibited shortened and misguided axons *in vivo* (Fig. 8E; Fig. 8G–I). In contrast, the expression of the TUBB3 control shRNA had no effect on commissural axons projection (Fig. 8D; Fig. 8G–I). As predicted, the expression of the wild-type RNAi-resistant human TUBB3 rescued the effects of TUBB3 RNAi knockdown on commissural axon extension and turning (Fig. 8F–I). These results indicate that TUBB3 is required for both the projection and pathfinding of commissural axons *in vivo* in the developing spinal cord.

Discussion

TUBB3 is the most dynamic β-tubulin isotype (Katsetos et al., 2003) and mutations in *TUBB3* result in neurological disorders associated with abnormal neuronal migration, differentiation and axon guidance (Poirier et al., 2010; Tischfield et al., 2010). Our results here indicate that TUBB3 interacts directly with DCC and is required for netrin-1-induced axon outgrowth and turning in the developing nervous system. These results not only untangle the role of TUBB3 in netrin signaling, but also provide a working model for the direct involvement of MT dynamics in axon guidance.

Fig. 6. Requirement of TUBB3 for netrin-1 attraction of spinal commissural axons. (**A**) Diagram of the *in ovo* electroporation and the co-culture assay with the open-book preparation. (**B**–**K′**) Electroporation of Venus YFP into the neural tube of chick embryos allowed visualization of axons. In the left panels (B,B′,D,D′,F,F′,H,H′,J,J′), neural tube explants were co-cultured with control HEK293 cells and commissural axons projected straight toward the floor plate (FP). In the right panels (C,C′,E,E′,G,G′,I,I′,K,K′), neural tube explants were co-cultured with aggregates of HEK293 cells secreting netrin-1. The neural tube was electroporated with Venus YFP alone (B,B′,C,C′); Venus YFP together with the TUBB3 siRNA pool (D,D′,E,E′); Venus YFP together with the control shRNA (F,F′,G,G′); Venus YFP with the TUBB3 shRNA (H,H′,I,I′) and Venus YFP with the TUBB3 shRNA plus the wild-type human RNAi-resistant TUBB3 (J,J′,K,K′). Expression of either TUBB3 siRNAs or shRNA inhibited commissural axon turning towards the netrin-1 source. The commissural axon turning defect of RNAi knockdown could be rescued by expressing RNAi-resistant TUBB3. (**L**) Quantification of axon turning. The numbers on the top of each bar indicate the numbers of explants tested in the corresponding groups. Data are mean ± s.e.m. from groups I–VI. ***$P<0.001$ (one-way ANOVA and Fisher LSD post-hoc comparisons). NS, not significant. Scale bar:100 μm.

Direct coupling of netrin–DCC signaling to MT dynamics

The neuronal cytoskeleton plays an essential role in axon outgrowth and pathfinding. Although most of the research has focused on the role of actin dynamics in growth cone protrusion, recent studies suggest that MTs also play an instructive role in growth cone steering (Buck and Zheng, 2002; Dent et al., 2004; Dent et al., 2011; Suter and Forscher, 2000; Tanaka and Sabry, 1995). However, whether MT dynamics are directly regulated by guidance cues is still unclear. In this study, we have found that TUBB3, the neuronal β-tubulin isotype III, colocalizes with DCC in the peripheral region, including both lamellipodia and filopodia, of the growth cones of developing commissural and cortical neurons (supplementary material Fig. S1). TUBB3 interacts directly with DCC and that netrin-1 induces these interactions both *in vitro* and *in vivo* (Fig. 1). The netrin-1-induced interaction of TUBB3 with DCC is abolished by the disruption of MT dynamics either with taxol or nocodazole, suggesting MT dynamics are required for these interactions (Fig. 2). DCC co-sediments with stabilized MTs and netrin-1 increases the ratio of DCC in the pellet versus the supernatant fraction (Fig. 2). Netrin-1 stimulation also increases the ratio of polymerized TUBB3 in the pellet. Live cell imaging of moving EB3 comets reveals that netrin-1 directly modulates MT dynamics in the growth cones of both primary E13 dorsal spinal cord (supplementary material Fig. S2; supplementary material Movies 1–4) and E15 cortical neurons (data not shown). More importantly, our functional data indicate that TUBB3 is required for netrin-1-induced MT dynamics (supplementary material Fig. S2; supplementary material Movies 1–4) as well as axon outgrowth and guidance both *in vitro* and *in vivo* (Figs 4–8). In addition, DCC intracellular P2–3 domain interacts with TUBB3 (Fig. 1I; supplementary material Fig. S5A,B) and this domain is required for netrin-1-induced neurite outgrowth and attraction (supplementary material Fig. S5C–I) (Gitai et al., 2003; Stein and Tessier-Lavigne, 2001; Stein et al., 2001). These results lead to a generalizable model suggesting netrin-1 signaling directly regulates MT dynamics through coupling its receptor DCC to TUBB3. In this model, in response to netrin-1, dynamic MTs are 'captured' by DCC in the growth cone, stabilizing filopodia against retraction and promoting axon outgrowth and turning. Previous studies on the role of MTs dynamics in the regulation of growth cone turning also support this model. For instance, 1) dynamic MTs became oriented and stabilized preferentially in the direction of the growth cone turn (Tanaka and Kirschner, 1995), 2) the local stabilization of MTs in one side of the growth cone caused the growth cone to turn towards that side (Buck and Zheng, 2002), 3) the local disruption of MT stabilization on one side of a growth cone was sufficient to induce growth cone turning away from that side (Buck and Zheng, 2002), 4) the application of low concentration of taxol enhanced axon outgrowth *in vitro* and *in vivo* via MT stabilization, promoting their polymerization at plus ends (Sengottuvel et al., 2011). These studies suggest that intrinsically polarized MT dynamics in the growth cone may be directly involved in axon guidance.

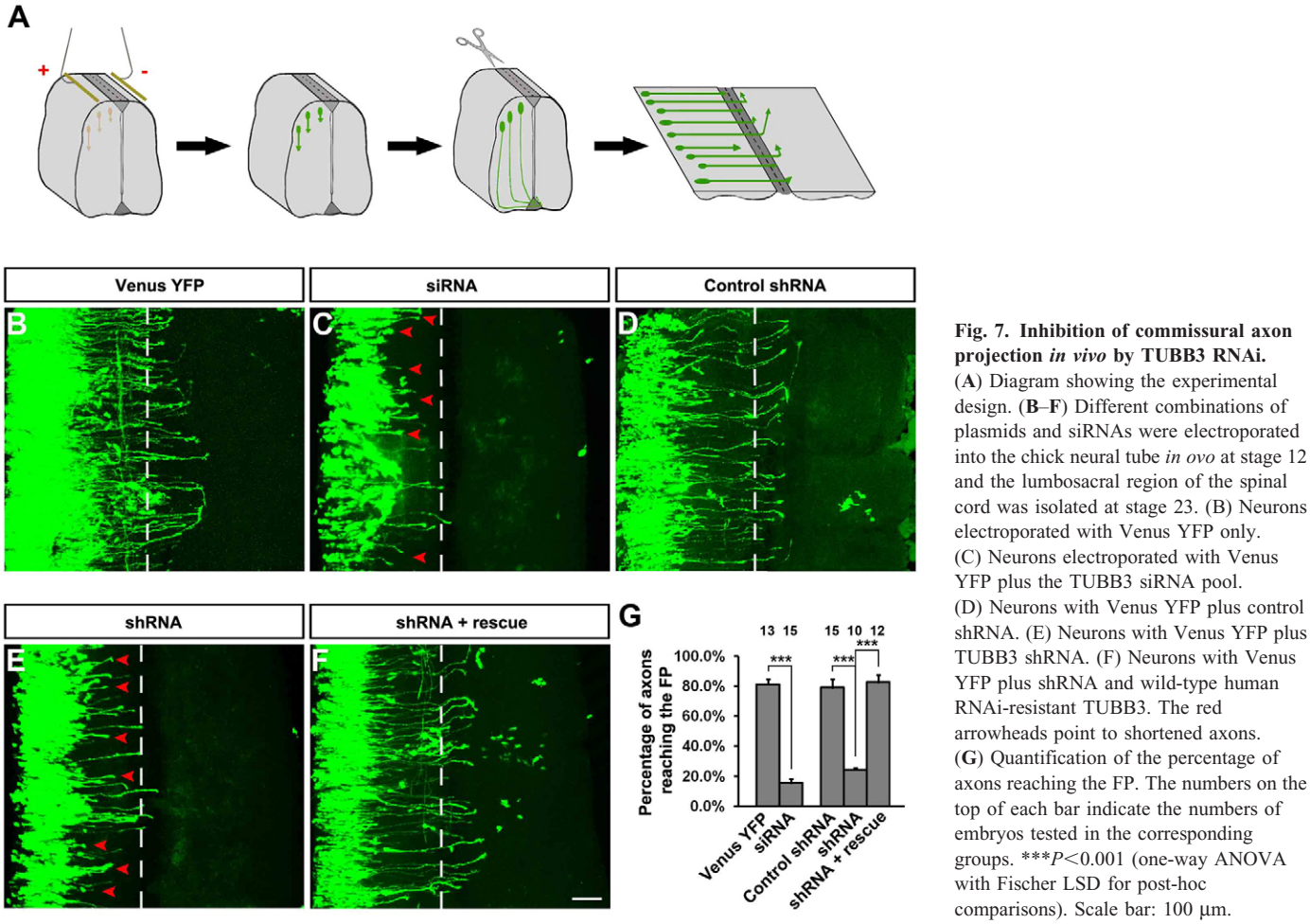

Fig. 7. Inhibition of commissural axon projection *in vivo* by TUBB3 RNAi. (**A**) Diagram showing the experimental design. (**B**–**F**) Different combinations of plasmids and siRNAs were electroporated into the chick neural tube *in ovo* at stage 12 and the lumbosacral region of the spinal cord was isolated at stage 23. (B) Neurons electroporated with Venus YFP only. (C) Neurons electroporated with Venus YFP plus the TUBB3 siRNA pool. (D) Neurons with Venus YFP plus control shRNA. (E) Neurons with Venus YFP plus TUBB3 shRNA. (F) Neurons with Venus YFP plus shRNA and wild-type human RNAi-resistant TUBB3. The red arrowheads point to shortened axons. (**G**) Quantification of the percentage of axons reaching the FP. The numbers on the top of each bar indicate the numbers of embryos tested in the corresponding groups. ***$P<0.001$ (one-way ANOVA with Fischer LSD for post-hoc comparisons). Scale bar: 100 μm.

TUBB3 is an essential downstream component coupling netrin-1 signaling to MT dynamics and to axon outgrowth and guidance

The spectrum of *TUBB3*-mutation phenotypes includes malformations of oculomotor nerves, the corpus callosum, anterior commissural, cortical spinal tracts and neuronal migration defects, suggesting that TUBB3 is required for axon guidance in the developing brain (Poirier et al., 2010; Tischfield et al., 2010). However, it is unclear why TUBB3 mutations are only associated with specific axon projection defects, such as those involved in commissural axon guidance, when it is widely expressed in all neurons in the developing nervous system. Although mutations in *TUBB3* result in the perturbation of MT dynamics (Poirier et al., 2010; Tischfield et al., 2010), the specific role of TUBB3 in axon guidance in the developing nervous system is unknown. In this study, we propose that TUBB3 plays an essential role in netrin-1 signaling, involved in netrin-1-promoted axon outgrowth and projection in the developing nervous system.

We have described a functional role of TUBB3 in netrin signaling both *in vitro* and *in vivo*. Netrin-1 increased neurite growth from primary cortical neurons and chick dorsal spinal cord explants (Figs 4 and 5), as reported in previous studies (Li et al., 2008; Liu et al., 2004; Liu et al., 2007; Liu et al., 2009). Both a TUBB3 siRNA pool and a specific TUBB3 shRNA inhibited neurite outgrowth induced by netrin-1 (Figs 4 and 5). In addition, TUBB3 knockdown by these same siRNA pool or shRNA also inhibited netrin-1-induced axon attraction in the chick open-book turning assay (Fig. 6). These results demonstrate that TUBB3 is involved in netrin-induced axon outgrowth and attraction *in vitro*. TUBB3 is also required for spinal commissural axon projection *in vivo*, as indicated by *in ovo* electroporation studies with chick spinal cords (Figs 7 and 8). Together, these studies strongly suggest that TUBB3 plays an essential role in netrin-1-mediated axon outgrowth and guidance in the developing nervous system.

TUBB3 mutations primarily affect MT function in a dominant fashion through altering heterodimer incorporation, MT stability, motor protein trafficking and kinesin-MT interactions (Tischfield et al., 2010). In future studies, it will be interesting to determine whether these *TUBB3* mutations can affect the netrin-1-dependent interaction of TUBB3 with DCC. Although DCC could not interact with TUBB1 and TUBB2, heterozygous missense mutations in TUBA1A and TUBB2B share certain phenotypic similarities in brain malformations, such as dysgenesis of the corpus callosum, basal ganglia dysmorphisms and neuronal migration defects, suggesting that these tubulin isotypes may have important overlapping functions (Jaglin et al., 2009; Keays et al., 2007; Poirier et al., 2010; Tischfield et al., 2010). It remains to be determined whether TUBA1A and TUBB2B can associate with other netrin receptors, such as DSCAM and UNC5C, in netrin signaling.

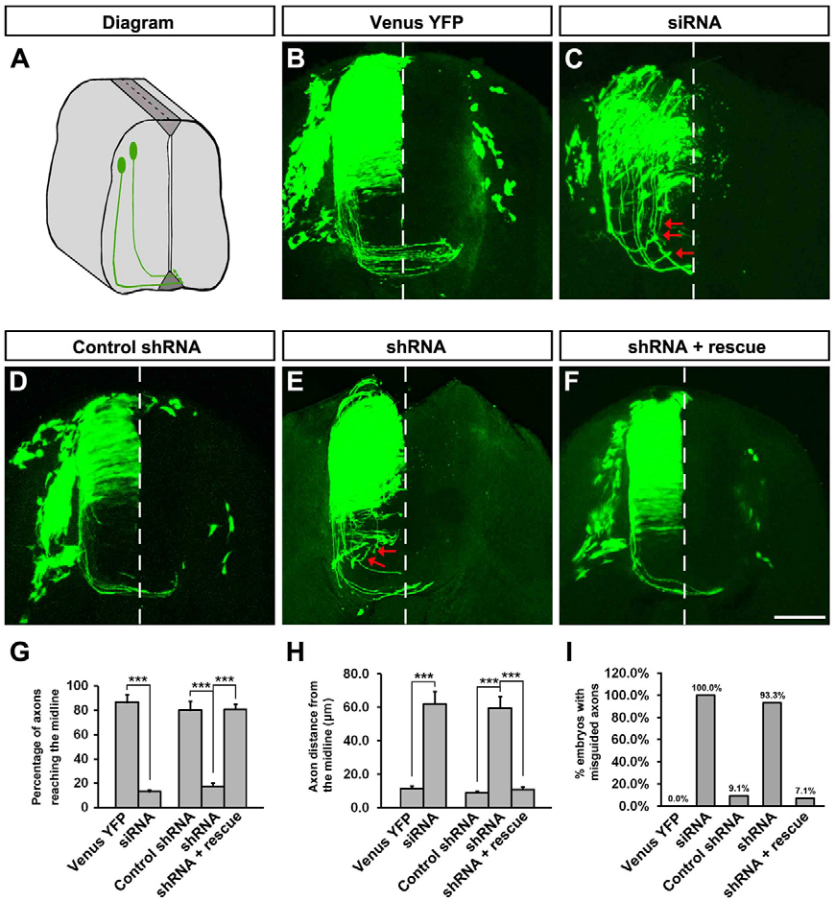

Fig. 8. TUBB3 is essential for spinal cord commissural axon pathfinding *in vivo*. (**A**) Diagram showing the transverse section of the chick spinal cord after electroporation. (**B**–**F**) The chick neural tube was electroporated with Venus YFP only (B), Venus YFP plus the TUBB3 siRNA pool (C), Venus YFP plus control shRNA (D), Venus YFP plus TUBB3 shRNA (E) or Venus YFP plus shRNA and wild-type human RNAi-resistant TUBB3 (F). Expression of TUBB3 siRNAs or shRNA not only inhibited the commissural axon extension but also caused aberrant pathfinding (C,E). The wild-type RNAi-resistant TUBB3 rescued the defect of TUBB3 shRNA knockdown on commissural axon projection and turning (F). The red arrows point to misguided axons. (**G**) Quantification of the percentage of axons reaching the midline of the chick spinal cord. (**H**) Quantification of the average distance of axons away from the midline. (**I**) The percentage of embryos with misguided axons. The numbers of embryos tested were 17 for the Venus YFP group, 14 for the siRNA pool group, 12 for the control shRNA group, 15 for the TUBB3 shRNA group and 14 for the rescue group. ***$P<0.001$ (one-way ANOVA with Fischer LSD for post-hoc comparisons). Scale bar: 100 μm.

Src family kinases are required for coupling netrin signaling to MT dynamics

Src family kinases are involved in netrin/DCC signaling (Li et al., 2004; Liu et al., 2004; Liu et al., 2007; Liu et al., 2009; Meriane et al., 2004). Netrin-1 can stimulate the tyrosine phosphorylation of TUBB3 by Src family kinases and this TUBB3 phosphorylation appears to be required for the subsequent interaction of TUBB3 with DCC and modulation of MT dynamics. For example, the inhibition of Src kinases by PP2, a Src family kinase inhibitor, 1) decreases netrin-1-induced TUBB3 phosphorylation (Fig. 3D; supplementary material Fig. S3B; Fig. 2) decreases the netrin-1-stimulated interaction of DCC with TUBB3 in primary neurons (Fig. 3E,F) blocks netrin-1-induced co-sedimentation of DCC with polymerized MT (Fig. 3G,H). Together, these results suggest that Src family kinases are essential in regulating MT dynamics in netrin-1 signaling and may function as a key signaling component of DCC/TUBB3 complex. Indeed, Src family kinases play an important role in growth cone steering via regulating MT dynamics (Suter et al., 2004). Therefore, these results suggest a model in which DCC serves as a signaling platform for recruitment of a multiprotein complex, including TUBB3, Src family kinases and other key signaling molecules to modulate MT dynamics in netrin-1-induced axon outgrowth and turning.

In addition to Src family kinases, many other signaling molecules have been identified in netrin/DCC signaling (Guan and Rao, 2003; Kolodkin and Tessier-Lavigne, 2011; Lai Wing Sun et al., 2011) including cyclic nucleotides, phospholipase C, phosphoinositol-3-kinase, mitogen-activated protein kinases, TRIO, DOCK180, transient receptor potential channels, calcium, myosin-X, PAK1 and Enabled/vasodilator-stimulated phosphoprotein. Whether these signaling molecules may also be involved in directly regulating MT dynamics through coupling netrin receptors to TUBB3 remains to be investigated.

It has long been recognized that the different signal transduction cascades initiated by extracellular guidance cues converge on the cytoskeleton to manipulate growth cone behavior (Buck and Zheng, 2002; Dent and Gertler, 2003; Dent et al., 2011; Lowery and Van Vactor, 2009; Vitriol and Zheng, 2012). The coordination of dynamic MTs and actin filaments in growth cones is necessary for proper axon outgrowth and guidance (Buck and Zheng, 2002; Dent and Gertler, 2003; Dent et al., 2011; Lowery and Van Vactor, 2009; Vitriol and Zheng, 2012). Although actin polymerization is not necessary for neurite outgrowth, the disruption of actin dynamics by cytochalasin D blocks growth cone turning induced by local taxol application, suggesting that the actin cytoskeleton plays an essential role in MT stabilization in growth cone turning (Buck and Zheng, 2002; Marsh and Letourneau, 1984). It will be interesting to investigate whether the interaction of DCC with TUBB3 will be regulated by actin dynamics, such as polymerization–depolymerization, treadmilling and retrograde flow in response to netrin signaling.

Materials and Methods

Materials

The following antibodies were used: rabbit anti-FLAG, mouse anti-phosphotyrosine antibody 4G10 (anti-pY) and rabbit anti-TUBB3 (Abcam, Cambridge, MA, USA); rabbit anti-MBP and rabbit anti-hemagglutinin (HA) (Santa Cruz, CA, USA); mouse anti-DCC (BD Biosciences, San Jose, CA, USA); mouse anti-TUBB3 (Covance, Princeton, New Jersey, USA); mouse anti-GST (Cell Signaling, Danvers, MA, USA); Alexa Fluor® 488 goat anti-mouse IgG and Alexa Fluor® 647 goat anti-rabbit IgG (Invitrogen, Grand Island, NY, USA); mouse anti-Myc, and mouse functional blocking anti-DCC (Calbiochem, Rockland, MA, USA). Taxol and nocodazole were obtained from MP Biochemicals (Solon, OH, USA). PP2 and PP3 were from Calbiochem. Purified TUBB3 was purchased from Origene (Rockville, MD, USA) and TUBB3-GST from Abnova (Walnut, CA, USA). Plasmids encoding TUBB3, DCC, DCC-ΔP1 (Δ1147–1170), ΔP2 (Δ1335–1356), and ΔP3 (Δ1412–1447) have been described previously (Li et al., 2004). The sequence-verified DCC intracellular P2–3 domain was subcloned into pT-Rex™-Dest 30 vector via Gateway technology (Invitrogen). TUBB3 ON-TARGETplus SMARTpool was obtained from Dharmacon (Waltham, MA, USA). The targeted sequences of control shRNA and DCC shRNA are: AATGCATCTCTGCAAGAGGTA and CATCCGATGTGCGACTGTA, respectively. The target sequence was inserted into pAVU6+27 between *Sal*I site and *Xba*I site. TUBB3 shRNA and control shRNA were gifts from David L. Turner (Yu et al., 2002), EB3-GFP constructs were from Niels Galjart and TUBB3-V5 were from Elizabeth C Engle. For TUBB3 RNAi rescue experiments, an RNAi-resistant construct was created by introducing seven silent point mutations in the target sequences.

Netrin-1 protein was either obtained from R&D (Minneapolis, MN, USA) or purified with anti-Myc tag affinity matrix from the conditioned media of HEK cells stably secreting netrin-1. The control was made by sham-purification from the conditioned media from HEK cells that had not been transfected with a cDNA expressing the Myc-tagged netrin-1. Recombinant DCC intracellular domain tagged with maltose-binding protein (DCC-ICD-MBP) was produced from BL21 competent *E. coli* and purified using amylose resin (New England Biolabs, Ipswich, MA, USA). The fusion protein was eluted with maltose and analyzed by SDS-PAGE, followed by Coomassie Blue staining.

Primary neuron cultures and nucleofection

The dissociated primary neuron culture and nucleofection procedures were performed as described previously (Liu et al., 2004; Liu et al., 2007; Liu et al., 2009). For examining the effect of RNAi knockdown, dissociated primary neurons were cultured on PLL-coated dishes for 2 days after nucleofection and cell lysates then analyzed by western blotting. For examining neurite outgrowth, cortical neurons were left settling on the coverslips for 2 hours and then cultured in DMEM with B27 (Invitrogen) and penicillin/streptomycin at 37℃ with 5% CO_2 for 20 hours with purified netrin-1 (250 ng/ml) or the sham-purified control. Cells were then fixed with 4% pre-warmed paraformaldehyde (PFA) for 20 minutes and stained with the Alexa Fluor® 555 phalloidin (Molecular Probes, Grand Island, NY, USA). Nuclei were visualized with Hoechst dye 33342 or DAPI (Invitrogen). Images were taken under a fluorescent microscope (Olympus IX81, Pittsburgh, PA, USA). The longest and total neurite length was examined using NIH ImageJ program.

Immunoprecipitation and western analysis

HEK293 cells were transfected with the PEI method and cultured 48 hours after transfection. For netrin-1 stimulation, primary neurons and transfected HEK293 cells were starved for 8 hours in serum-free DMEM media and followed by incubation with purified netrin-1 protein (500 ng/ml) or sham purified control up to 30 minutes. For immunoprecipitation, primary neurons from E15 mouse cortex, E13 dorsal spinal cord and HEK293 cells were lysed as described previously (Li et al., 2008; Liu et al., 2004; Liu et al., 2007; Liu et al., 2009). Cell lysates were incubated with specific antibodies for 2 hours before protein A/G-agarose beads (Santa Cruz Biotechnology) were added. For the immunoblotting, protein extracts were separated with 7.5% SDS-PAGE and western blots were visualized with the enhanced chemiluminescence kit (Fisher, Pittsburgh, PA, USA).

Microtubule co-sedimentation assay

E15 mouse cortical neurons were dissociated and cultured as previously described (Li et al., 2008; Liu et al., 2004; Liu et al., 2007; Liu et al., 2009). Primary neurons were stimulated by purified netrin-1 (500 ng/ml) or sham-purified control for 20 minutes. To detect the effects of Src family kinases on MT dynamics, PP2 (5 nM) or PP3 (5 nM) was added 6 hours before netrin-1 stimulation. Primary neurons were lysed in the MLB buffer and cell lysates centrifuged at 100,000×***g*** for 1 hour at 4℃. The supernatant was incubated with 40 μM taxol or DMSO in PEMG buffer (100 mM PIPES, 1 mM EGTA, 1 mM $MgSO_4$, 1 mM GTP, pH 6.8) at room temperature for 30 minutes. MTs were pelleted by centrifugation through a 10% sucrose cushion at 50,000×***g*** for 30 minutes at 4℃. The pellet and supernatant fractions were collected separately, and the pellet was resuspended with tubulin buffer (50 mM HEPES, 1 mM $MgCl_2$, 1 mM EGTA, 10% glycerol, 150 mM KCl, 40 μM taxol, 1 mM GTP, 5 mM Mg-ATP, 1 mM PMSF, 1× protease inhibitor mixture). Proteins in the supernatant and the pellet were separated by SDS-PAGE and analyzed by western blotting.

Immunocytochemistry

Dissociated neurons from E15 mouse cortexes and E11 dorsal spinal cords were fixed either in pre-warmed 4% PFA in 1×stabilization buffer (127 mM NaCl, 5 mM KCl, 1.1 mM NaH_2PO_4, 0.4 mM KH_2PO_4, 2 mM $MgCl_2$, 5.5 mM glucose, 1 mM EGTA, 10 mM PIPES) or ice-cold methanol and permeabilized with 0.5% Triton X-100 for 15 minutes. Cells were blocked with 0.25% BSA and 0.1% Triton in PBS at room temperature for 30 minutes and then incubated with primary antibody solution containing mouse anti-DCC (1:100) and rabbit anti-TUBB3 (1:300) antibodies overnight at 4℃. Neurons were incubated with secondary antibodies (anti-mouse-488 and anti-rabbit-647) and mounted onto glass slides with Fluorogel (Electron Microscopy Sciences). Images of growth cones were taken sequentially using a confocal microscope (Olympus IX71 Fluoview, Pittsburgh, PA, USA) with the same exposure settings.

Chick spinal cord explant culture and analysis of axon outgrowth

Fertilized White Leghorn chicken eggs were incubated and chicken embryos staged as described previously (Liu et al., 2004; Liu et al., 2007; Liu et al., 2009). At stage 12–15, plasmids or siRNAs plus Venus YFP were injected into the neural tube of chicken embryos and the *in ovo* electroporation was performed with the following program: 25 V, 5 milliseconds, five pulses (BTX ECM830, Holliston, MA, USA) (Liu et al., 2004; Liu et al., 2007; Liu et al., 2009). Embryos at stage 18–20 were collected and examined under a fluorescent microscope. The dorsal one-third of the spinal cord labeled with YFP fluorescence was isolated, trimmed to 200 μm in size, and transferred into the mixed gel (3:2:1 collagen: matrigel: medium) as described previously (Liu et al., 2009). After gel polymerization, explants were cultured in DMEM with B27 (Invitrogen) and penicillin/streptomycin at 37℃ with 5% CO_2 overnight with purified netrin-1 (250 ng/ml) or the sham-purified control. Explants were fixed with 4% PFA in 1×PBS, and the images of axons with YFP fluorescence were obtained under a confocal microscope (Olympus IX70). The numbers of axons and total axon length per explant were measured using the NIH ImageJ software.

Chicken commissural axon turning assay

The *in ovo* electroporation procedures were essentially done as described above (Liu et al., 2004; Liu et al., 2007; Liu et al., 2009; Qu et al., 2013). Embryos were harvested at stages 18–20 and samples showing YFP fluorescence were isolated under the fluorescence microscope. The spinal cord was opened at the roof plate (open-book preparation) and explants from the half spinal cord with YFP fluorescence were co-cultured with an aggregate of control or netrin-1 secreting HEK cells as described previously (Liu et al., 2004; Liu et al., 2007; Liu et al., 2009). Axons with the turning angle towards the cell aggregate more than 5° were counted as attraction and the percentage of attractive axons was calculated from the numbers of fluorescent axons turning towards the HEK cell aggregate divided by the total numbers of fluorescent axons within 300 μm of the HEK cell aggregates. Images were acquired under an Olympus IX70 confocal microscope.

Chicken commissural axon projection *in vivo*

Chick spinal cords with YFP fluorescence were collected until stage 23 after electroporation as described previously (Li et al., 2008; Liu et al., 2007; Liu et al., 2009; Qu et al., 2013). The lumbosacral region of the spinal cord was isolated and the open-book preparation of the spinal cord was performed by opening the roof plate. After fixation, the tissues in the open-book preparation were mounted in Gel/Mount (Biomeda, Pittsburgh, MA, USA) for analysis of commissural axon projection *in vivo*. Images were taken under the confocal microscope. The percentage of axons reaching the floor plate was calculated from the numbers of fluorescent axons crossing the ipsilateral floor plate divided by the total numbers of fluorescent axons within 100 μm from the floor plate (Li et al., 2008; Liu et al., 2007; Liu et al., 2009).

To examine commissural axon pathfinding *in vivo*, the lumbosacral segments of the chick spinal cords expressing YFP at stage 23 were isolated and transverse sections of 200 μm were cut by a vibrotome. The spinal cord slices were mounted in Gel/Mount for confocal fluorescent microscopy. The percentage of axons reaching the midline was quantified from the numbers of fluorescent axons arriving at or crossing over the midline divided by the total numbers of fluorescent axons within 200 μm from the floor plate. The axon distance from the midline was calculated from the average distance of fluorescent axons away from the midline.

Acknowledgements

We thank Dr Andrea L. Kalinoski for help with confocal imaging, Dr David L. Turner for TUBB3 shRNA constructs, Dr Niels Galjart for EB3-GFP constructs, Dr Elizabeth C. Engle for TUBB3-V5 constructs, Dr Bruce Bamber for image analysis and Dr Richard

Komuniecki for comments on the manuscript. The authors declare no competing financial interests.

Author contributions

G.L. designed research; C.Q., T.D., Q.S., T.Y., H.H. and G.L. performed research; C.Q., T.D. and G.L. analyzed data; and G.L. wrote the paper.

Funding

We thank the Whitehall Foundation and the National Institutes of Health for support. Deposited in PMC for release after 12 months.

Supplementary material available online at
http://jcs.biologists.org/lookup/suppl/doi:10.1242/jcs.122184/-/DC1

References

Ackerman, S. L., Kozak, L. P., Przyborski, S. A., Rund, L. A., Boyer, B. B. and Knowles, B. B. (1997). The mouse rostral cerebellar malformation gene encodes an UNC-5-like protein. *Nature* **386**, 838-842.

Alcántara, S., Ruiz, M., De Castro, F., Soriano, E. and Sotelo, C. (2000). Netrin 1 acts as an attractive or as a repulsive cue for distinct migrating neurons during the development of the cerebellar system. *Development* **127**, 1359-1372.

Buck, K. B. and Zheng, J. Q. (2002). Growth cone turning induced by direct local modification of microtubule dynamics. *J. Neurosci.* **22**, 9358-9367.

Colamarino, S. A. and Tessier-Lavigne, M. (1995). The axonal chemoattractant netrin-1 is also a chemorepellent for trochlear motor axons. *Cell* **81**, 621-629.

Dent, E. W. and Gertler, F. B. (2003). Cytoskeletal dynamics and transport in growth cone motility and axon guidance. *Neuron* **40**, 209-227.

Dent, E. W., Barnes, A. M., Tang, F. and Kalil, K. (2004). Netrin-1 and semaphorin 3A promote or inhibit cortical axon branching, respectively, by reorganization of the cytoskeleton. *J. Neurosci.* **24**, 3002-3012.

Dent, E. W., Gupton, S. L. and Gertler, F. B. (2011). The growth cone cytoskeleton in axon outgrowth and guidance. *Cold Spring Harb. Perspect. Biol.* **3**.

Fazeli, A., Dickinson, S. L., Hermiston, M. L., Tighe, R. V., Steen, R. G., Small, C. G., Stoeckli, E. T., Keino-Masu, K., Masu, M., Rayburn, H. et al. (1997). Phenotype of mice lacking functional Deleted in colorectal cancer (Dcc) gene. *Nature* **386**, 796-804.

Finger, J. H., Bronson, R. T., Harris, B., Johnson, K., Przyborski, S. A. and Ackerman, S. L. (2002). The netrin 1 receptors Unc5h3 and Dcc are necessary at multiple choice points for the guidance of corticospinal tract axons. *J. Neurosci.* **22**, 10346-10356.

Gitai, Z., Yu, T. W., Lundquist, E. A., Tessier-Lavigne, M. and Bargmann, C. I. (2003). The netrin receptor UNC-40/DCC stimulates axon attraction and outgrowth through enabled and, in parallel, Rac and UNC-115/AbLIM. *Neuron* **37**, 53-65.

Guan, K. L. and Rao, Y. (2003). Signalling mechanisms mediating neuronal responses to guidance cues. *Nat. Rev. Neurosci.* **4**, 941-956.

Hedgecock, E. M., Culotti, J. G. and Hall, D. H. (1990). The unc-5, unc-6, and unc-40 genes guide circumferential migrations of pioneer axons and mesodermal cells on the epidermis in C. elegans. *Neuron* **4**, 61-85.

Hong, K., Hinck, L., Nishiyama, M., Poo, M. M., Tessier-Lavigne, M. and Stein, E. (1999). A ligand-gated association between cytoplasmic domains of UNC5 and DCC family receptors converts netrin-induced growth cone attraction to repulsion. *Cell* **97**, 927-941.

Ishii, N., Wadsworth, W. G., Stern, B. D., Culotti, J. G. and Hedgecock, E. M. (1992). UNC-6, a laminin-related protein, guides cell and pioneer axon migrations in C. elegans. *Neuron* **9**, 873-881.

Jaglin, X. H., Poirier, K., Saillour, Y., Buhler, E., Tian, G., Bahi-Buisson, N., Fallet-Bianco, C., Phan-Dinh-Tuy, F., Kong, X. P., Bomont, P. et al. (2009). Mutations in the beta-tubulin gene TUBB2B result in asymmetrical polymicrogyria. *Nat. Genet.* **41**, 746-752.

Kalil, K. and Dent, E. W. (2005). Touch and go: guidance cues signal to the growth cone cytoskeleton. *Curr. Opin. Neurobiol.* **15**, 521-526.

Katsetos, C. D., Legido, A., Perentes, E. and Mörk, S. J. (2003). Class III beta-tubulin isotype: a key cytoskeletal protein at the crossroads of developmental neurobiology and tumor neuropathology. *J. Child Neurol.* **18**, 851-866, discussion 867.

Keays, D. A., Tian, G., Poirier, K., Huang, G.-J., Siebold, C., Cleak, J., Oliver, P. L., Fray, M., Harvey, R. J., Molnár, Z. et al. (2007). Mutations in alpha-tubulin cause abnormal neuronal migration in mice and lissencephaly in humans. *Cell* **128**, 45-57.

Keeling, S. L., Gad, J. M. and Cooper, H. M. (1997). Mouse Neogenin, a DCC-like molecule, has four splice variants and is expressed widely in the adult mouse and during embryogenesis. *Oncogene* **15**, 691-700.

Keino-Masu, K., Masu, M., Hinck, L., Leonardo, E. D., Chan, S. S., Culotti, J. G. and Tessier-Lavigne, M. (1996). Deleted in Colorectal Cancer (DCC) encodes a netrin receptor. *Cell* **87**, 175-185.

Kennedy, T. E., Serafini, T., de la Torre, J. R. and Tessier-Lavigne, M. (1994). Netrins are diffusible chemotropic factors for commissural axons in the embryonic spinal cord. *Cell* **78**, 425-435.

Kolodkin, A. L. and Tessier-Lavigne, M. (2011). Mechanisms and molecules of neuronal wiring: a primer. *Cold Spring Harb. Perspect. Biol.* **3**.

Kolodziej, P. A., Timpe, L. C., Mitchell, K. J., Fried, S. R., Goodman, C. S., Jan, L. Y. and Jan, Y. N. (1996). frazzled encodes a Drosophila member of the DCC immunoglobulin subfamily and is required for CNS and motor axon guidance. *Cell* **87**, 197-204.

Lai Wing Sun, K., Correia, J. P. and Kennedy, T. E. (2011). Netrins: versatile extracellular cues with diverse functions. *Development* **138**, 2153-2169.

Leonardo, E. D., Hinck, L., Masu, M., Keino-Masu, K., Ackerman, S. L. and Tessier-Lavigne, M. (1997). Vertebrate homologues of C. elegans UNC-5 are candidate netrin receptors. *Nature* **386**, 833-838.

Li, W., Lee, J., Vikis, H. G., Lee, S. H., Liu, G., Aurandt, J., Shen, T. L., Fearon, E. R., Guan, J. L., Han, M. et al. (2004). Activation of FAK and Src are receptor-proximal events required for netrin signaling. *Nat. Neurosci.* **7**, 1213-1221.

Li, X., Gao, X., Liu, G., Xiong, W., Wu, J. and Rao, Y. (2008). Netrin signal transduction and the guanine nucleotide exchange factor DOCK180 in attractive signaling. *Nat. Neurosci.* **11**, 28-35.

Liu, G., Beggs, H., Jürgensen, C., Park, H. T., Tang, H., Gorski, J., Jones, K. R., Reichardt, L. F., Wu, J. and Rao, Y. (2004). Netrin requires focal adhesion kinase and Src family kinases for axon outgrowth and attraction. *Nat. Neurosci.* **7**, 1222-1232.

Liu, G., Li, W., Gao, X., Li, X., Jürgensen, C., Park, H. T., Shin, N. Y., Yu, J., He, M. L., Hanks, S. K. et al. (2007). p130CAS is required for netrin signaling and commissural axon guidance. *J. Neurosci.* **27**, 957-968.

Liu, G., Li, W., Wang, L., Kar, A., Guan, K. L., Rao, Y. and Wu, J. Y. (2009). DSCAM functions as a netrin receptor in commissural axon pathfinding. *Proc. Natl. Acad. Sci. USA* **106**, 2951-2956.

Lowery, L. A. and Van Vactor, D. (2009). The trip of the tip: understanding the growth cone machinery. *Nat. Rev. Mol. Cell Biol.* **10**, 332-343.

Ly, A., Nikolaev, A., Suresh, G., Zheng, Y., Tessier-Lavigne, M. and Stein, E. (2008). DSCAM is a netrin receptor that collaborates with DCC in mediating turning responses to netrin-1. *Cell* **133**, 1241-1254.

Marsh, L. and Letourneau, P. C. (1984). Growth of neurites without filopodial or lamellipodial activity in the presence of cytochalasin B. *J. Cell Biol.* **99**, 2041-2047.

Meriane, M., Tcherkezian, J., Webber, C. A., Danek, E. I., Triki, I., McFarlane, S., Bloch-Gallego, E. and Lamarche-Vane, N. (2004). Phosphorylation of DCC by Fyn mediates Netrin-1 signaling in growth cone guidance. *J. Cell Biol.* **167**, 687-698.

Poirier, K., Saillour, Y., Bahi-Buisson, N., Jaglin, X. H., Fallet-Bianco, C., Nabbout, R., Castelnau-Ptakhine, L., Roubertie, A., Attie-Bitach, T., Desguerre, I. et al. (2010). Mutations in the neuronal ß-tubulin subunit TUBB3 result in malformation of cortical development and neuronal migration defects. *Hum. Mol. Genet.* **19**, 4462-4473.

Purohit, A. A., Li, W., Qu, C., Dwyer, T., Shao, Q., Guan, K.-L. and Liu, G. (2012). Down syndrome cell adhesion molecule (DSCAM) associates with uncoordinated-5C (UNC5C) in netrin-1-mediated growth cone collapse. *J. Biol. Chem.* **287**, 27126-27138.

Qu, C., Li, W., Shao, Q., Dwyer, T., Huang, H., Yang, T. and Liu, G. (2013). c-Jun N-terminal kinase 1 (JNK1) is required for coordination of netrin signaling in axon guidance. *J. Biol. Chem.* **288**, 1883-1895.

Sbalzarini, I. F. and Koumoutsakos, P. (2005). Feature point tracking and trajectory analysis for video imaging in cell biology. *J. Struct. Biol.* **151**, 182-195.

Sengottuvel, V., Leibinger, M., Pfreimer, M., Andreadaki, A. and Fischer, D. (2011). Taxol facilitates axon regeneration in the mature CNS. *J. Neurosci.* **31**, 2688-2699.

Serafini, T., Kennedy, T. E., Galko, M. J., Mirzayan, C., Jessell, T. M. and Tessier-Lavigne, M. (1994). The netrins define a family of axon outgrowth-promoting proteins homologous to C. elegans UNC-6. *Cell* **78**, 409-424.

Serafini, T., Colamarino, S. A., Leonardo, E. D., Wang, H., Beddington, R., Skarnes, W. C. and Tessier-Lavigne, M. (1996). Netrin-1 is required for commissural axon guidance in the developing vertebrate nervous system. *Cell* **87**, 1001-1014.

Stein, E. and Tessier-Lavigne, M. (2001). Hierarchical organization of guidance receptors: silencing of netrin attraction by slit through a Robo/DCC receptor complex. *Science* **291**, 1928-1938.

Stein, E., Zou, Y., Poo, M. and Tessier-Lavigne, M. (2001). Binding of DCC by netrin-1 to mediate axon guidance independent of adenosine A2B receptor activation. *Science* **291**, 1976-1982.

Suter, D. M. and Forscher, P. (2000). Substrate-cytoskeletal coupling as a mechanism for the regulation of growth cone motility and guidance. *J. Neurobiol.* **44**, 97-113.

Suter, D. M., Schaefer, A. W. and Forscher, P. (2004). Microtubule dynamics are necessary for SRC family kinase-dependent growth cone steering. *Curr. Biol.* **14**, 1194-1199.

Tanaka, E. and Kirschner, M. W. (1995). The role of microtubules in growth cone turning at substrate boundaries. *J. Cell Biol.* **128**, 127-137.

Tanaka, E. and Sabry, J. (1995). Making the connection: cytoskeletal rearrangements during growth cone guidance. *Cell* **83**, 171-176.

Tessier-Lavigne, M., Placzek, M., Lumsden, A. G., Dodd, J. and Jessell, T. M. (1988). Chemotropic guidance of developing axons in the mammalian central nervous system. *Nature* **336**, 775-778.

Tischfield, M. A., Baris, H. N., Wu, C., Rudolph, G., Van Maldergem, L., He, W., Chan, W. M., Andrews, C., Demer, J. L., Robertson, R. L. et al. (2010). Human TUBB3 mutations perturb microtubule dynamics, kinesin interactions, and axon guidance. *Cell* **140**, 74-87.

Vitriol, E. A. and Zheng, J. Q. (2012). Growth cone travel in space and time: the cellular ensemble of cytoskeleton, adhesion, and membrane. *Neuron* **73**, 1068-1081.

Yu, J.-Y., DeRuiter, S. L. and Turner, D. L. (2002). RNA interference by expression of short-interfering RNAs and hairpin RNAs in mammalian cells. *Proc. Natl. Acad. Sci. USA* **99**, 6047-6052.

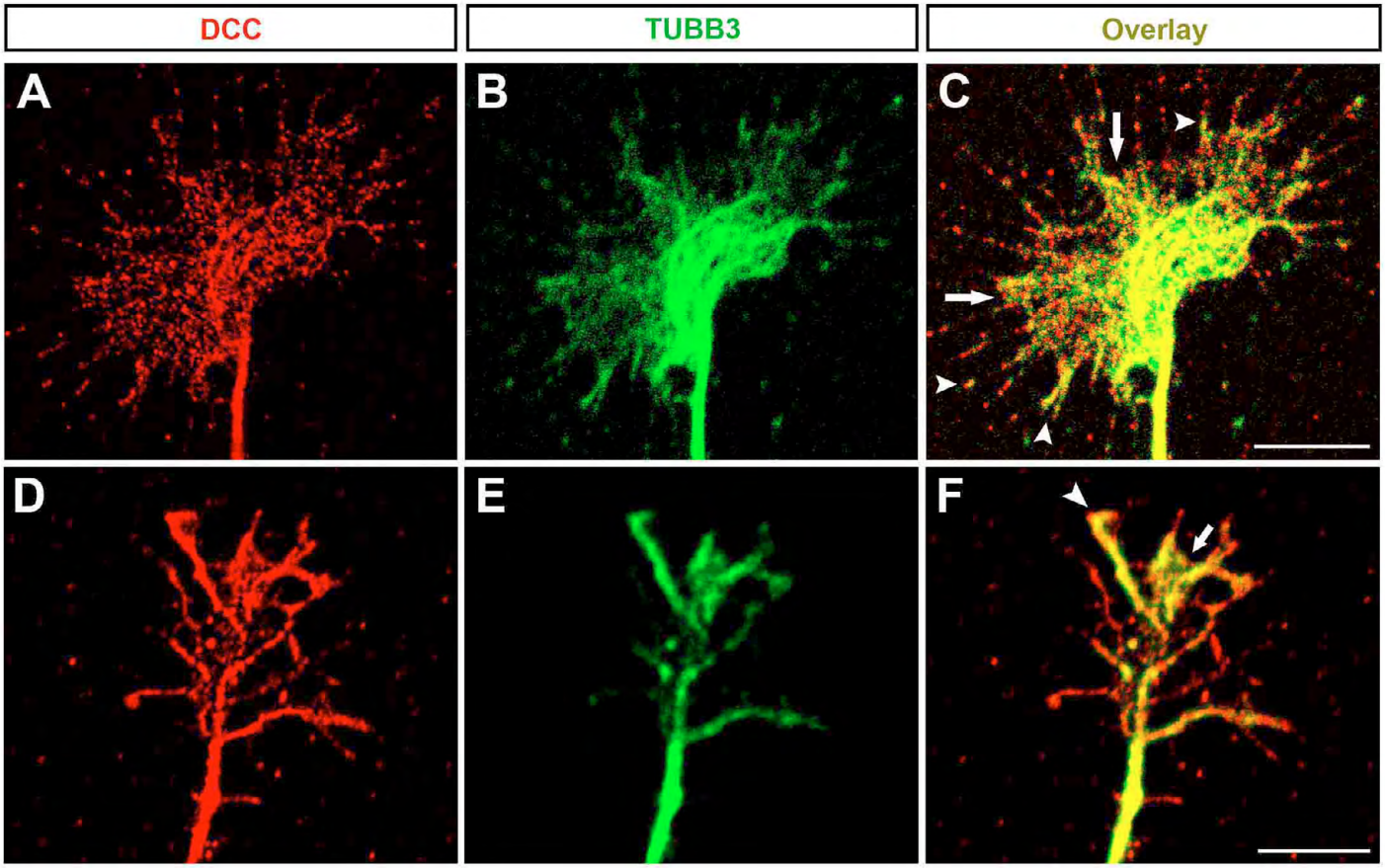

Fig. S1. Subcellular colocalization of DCC with TUBB3 in the growth cone of primary neurons. (**A–C**) Localization of DCC (A) and TUBB3 (B) in dissociated commissural neurons from E11 mouse spinal cords cultured for 4 days. Panel C is merged images of A and B. Quantitative analysis of fluorescence colocalization was performed on original images (Volocity, Version 4.0, Improvision, Waltham, MD, USA). Background was corrected and a free-hand ROI was drawn around the outer edge of the growth cone including lamellipodia and filopodia, but excluding the central core area where pixel intensities tended to be saturated. To evaluate the degree of colocalization of green and red fluorescence within the specified ROI, Pearson's Correlation Coefficient, r, was calculated using the colocalization module in Volocity (means ± S.D.). The value of Pearson's correlation coefficient in A–C was 0.71 ± 0.08. (**D–F**) DCC colocalized with TUBB3 in the growth cones of dissociated cortical neurons from E15 mouse cortexes cultured for 4 days. Panel F is merged images of D and E. The value of Pearson's correlation coefficient of DCC and TUBB3 in the P region of growth cones in D–F was 0.74 ± 0.07. White arrowheads, examples of colocalization sites of DCC and TUBB3 in filopodia; White arrows, examples of overlap in lamellipoda. Scale bars: 10 μm.

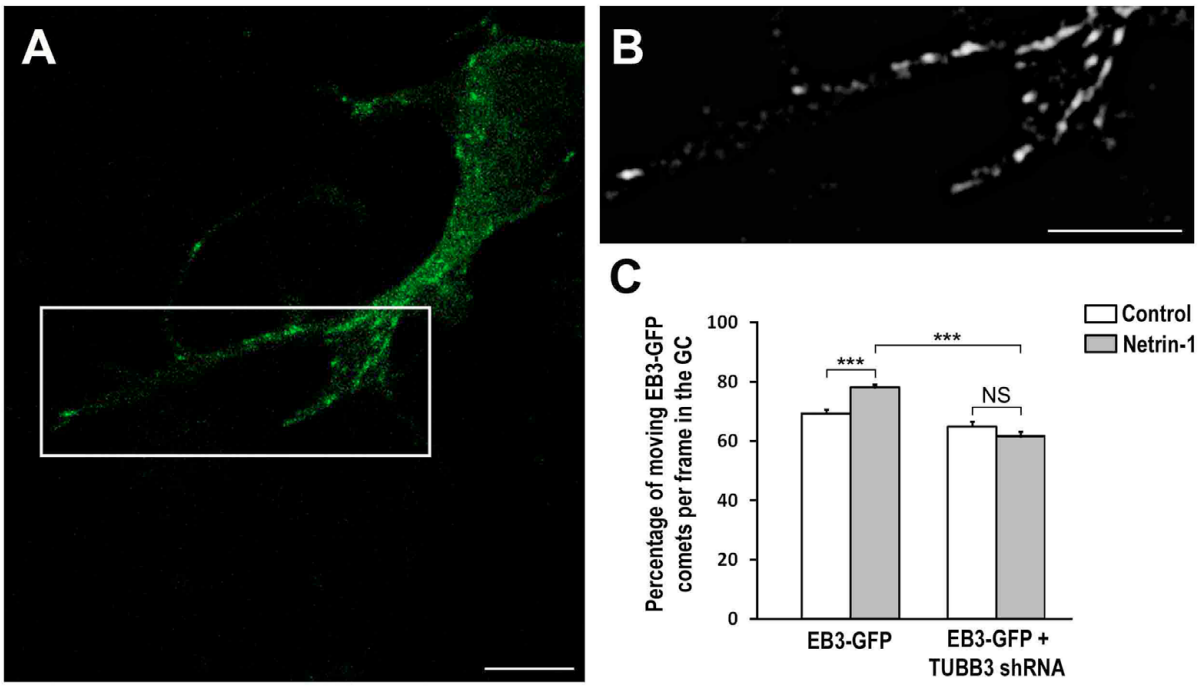

Fig. S2. Time-lapse recording of EB3-GFP in dissociated E13 dorsal spinal cord neurons. (**A**) EB3-GFP comets in transfected spinal cord neurons. E13 dorsal spinal cord neurons were dissociated and nucleofected with EB3-GFP. Primary neurons were cultured for 1–3 days before live imaging in a 37°C chamber using a Leica TCS SP8 confocal microscope (Leica Microsystems Inc., Buffalo Grove, IL). Images were acquired every 1–4 s over 60 frames per growth cone and were corrected for photobleaching and background subtraction. The box in A represents the growth cone in the EB3-GFP-transfected neuron and is magnified in B. (**B**) Images were passed through a bandpass filter before particle detection and trajectories of EB3-GFP comets in the growth cone (GC) using the Particle Tracker plugin for ImageJ (Sbalzarini and Koumoutsakos, 2005). (**C**) Quantification of the percentage of moving EB3-GFP comets to total EB3-GFP per frame in the growth cone of E13 dorsal spinal cord neurons (see supplementary material Movies 1–4). Primary neurons transfected with either EB3-GFP only or EB3-GFP and TUBB3 shRNA together were imaged with or without netrin-1 stimulation (200 ng/ml). Only comets that could be tracked for more than 3 frames were considered moving comets. Data are reported as mean ± s.e.m (2 growth cones in each group). NS, not significant; ***, $P<0.001$ (One-way ANOVA with Tamhane's T2 for post-hoc comparisons). GC, growth cone. Scale bars: 5 μm.

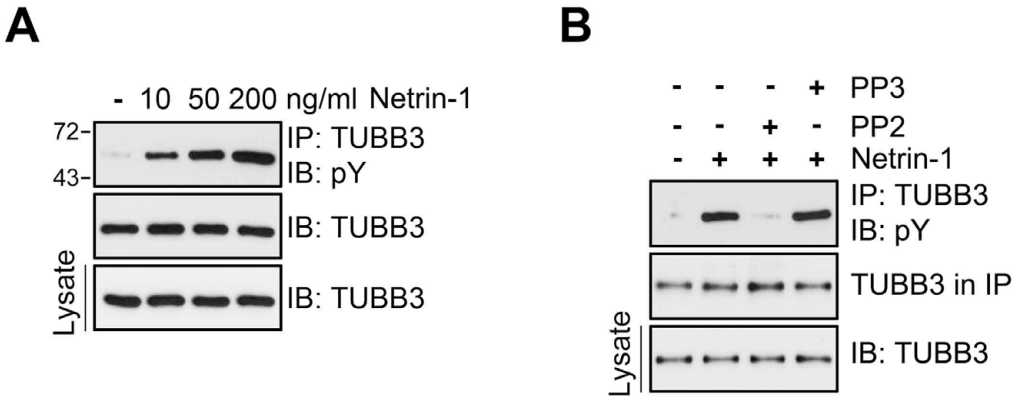

Fig. S3. Src family kinase activity is required for netin-1-induced TUBB3 tyrosine phosphorylation, related to Fig. 3B,D. (**A**) Netrin-1 induces tyrosine phosphorylation of endogenous TUBB3 in dissociated E15 cortical neurons (the reciprocal IP for Fig. 3B). TUBB3 was immunoprecipitated using anti-TUBB3 and the membrane was blotted for tyrosine phosphorylation using anti-pY. Primary neurons were stimulated with purified netrin-1 (200 ng/ml). (**B**) The induction of TUBB3 tyrosine phosphorylation by netrin-1 was inhibited by PP2, not PP3 (the reciprocal IP for Fig. 3D). Primary E15 cortical neurons were treated with purified netrin-1 (200 ng/ml) in the presence of PP2 or PP3.

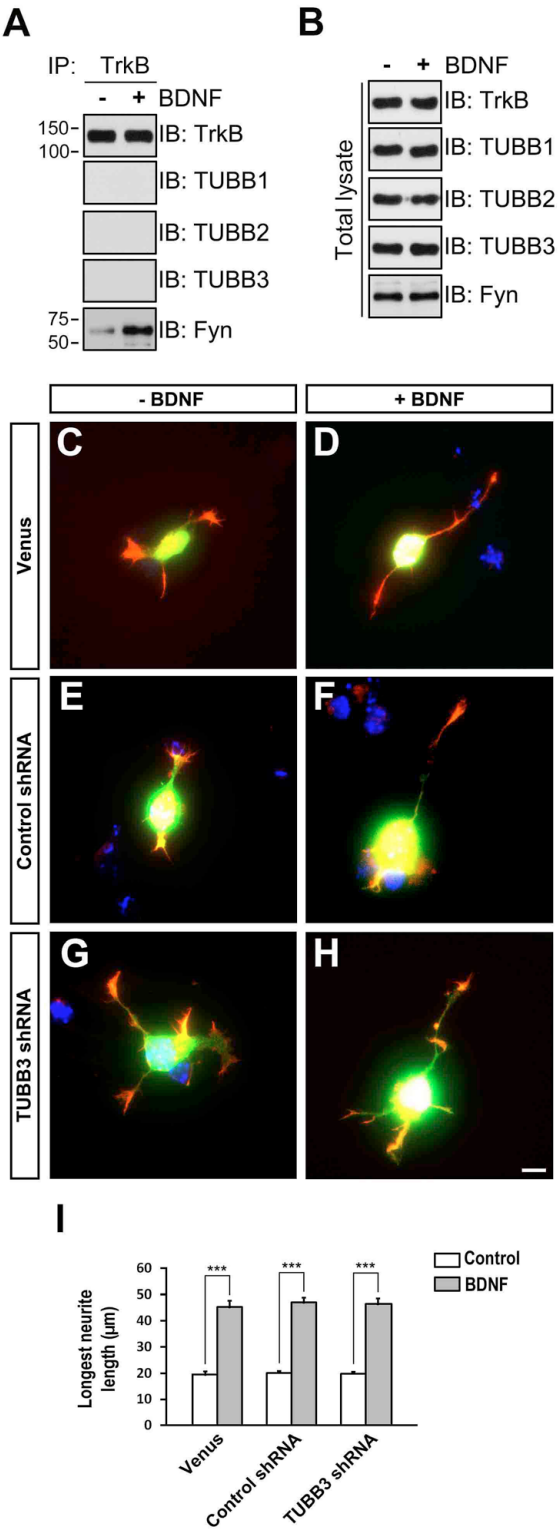

Fig. S4. TUBB3 could not bind to endogenous TrkB, a BDNF receptor, and was not involved in BDNF-promoted neurite outgrowth. (**A**,**B**) TrkB did not form protein–protein interaction complexes with TUBB1, TUBB2 and TUBB3 in primary cortical neurons with or without purified BDNF treatment. In contrast, the interaction of endogenous TrkB with Fyn was increased by BDNF stimulation. The anti-TrkB antibody was used to immunoprecipitate proteins and the blot was analyzed with anti-TUBB1, anti-TUBB2, anti-TUBB3 or anti-Fyn. Equivalent amounts of input TrkB, TUBB1, TUBB2, TUBB3 and Fyn in cortical lysates (B). (**C–I**) Cortical neurons from E15 mouse embryos were transfected with either Venus YFP only (C,D), Venus YFP plus TUBB3 control siRNA (E,F) or TUBB3 shRNA (G,H), respectively, and then cultured on coverslips coated with PLL. Neurons were cultured after 40 h and stained with the Alexa Fluor® 555 phalloidin and DAPI. Purified BDNF (50 ng/ml) induced the neurite outgrowth from YFP-positive neurons transfected with Venus YFP only (C,D) and Venus YFP plus control siRNA (E,F). Expression of TUBB3 shRNA did not affect BDNF-induced neurite outgrowth (G,H). (I) Quantification of the length of the longest neurite from individual neuron. The neurites of YFP-positive neurons not in contact with other neurons were quantified and used in the statistical analyses. Data are reported as mean ± s.e.m. ***, $P<0.001$ (One-way ANOVA with Fischer LSD for post-hoc comparisons). Scale bar: 10 μm.

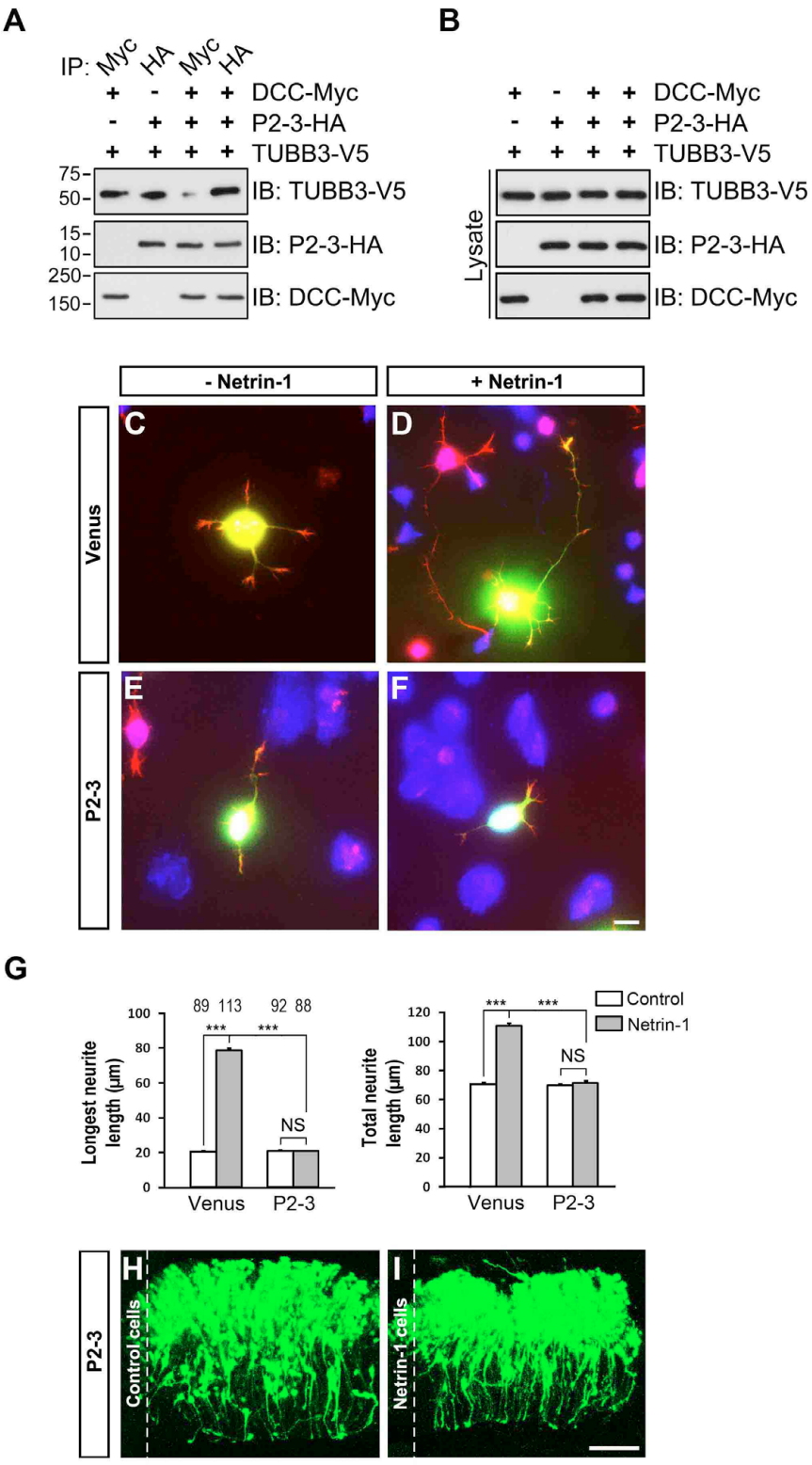

Fig. S5. The DCC intracellular P2-3 domain inhibited the interaction of TUBB3 with full-length wild-type DCC as well as netrin-1-induced neurite outgrowth and commissural axon attraction. (**A**,**B**) TUBB3-V5 were co-transfected with either wild-type full-length DCC-Myc, DCC P2-3-HA or full-length DCC-Myc and DCC P2-3-HA together into HEK293 cells. Cell lysates were immunoprecipitated using either anti-Myc or anti-HA and the membrane was blotted for TUBB3 using anti-V5. (B) Equivalent amounts of input TUBB3-V5, DCC P2-3-HA and DCC-Myc. (**C–G**) Expression of DCC P2-3 domain inhibited netrin-1-induced neurite outgrowth of cortical neurons. E15 mouse cortical neurons were transfected with either Venus YFP only (C,D) or Venus YFP plus DCC P2-3 (E,F). Primary neurons were treated with either purified netrin-1 (D,F) or the sham-purified control (C,E). (G) Quantification of netrin-1-induced neurite outgrowth. The numbers on the top of each bar indicate the numbers of neurons tested in the corresponding groups. Data are mean ± s.e.m. NS, not significant; ***, $P<0.001$ (One-way ANOVA with Fischer LSD for post-hoc comparisons). (**H**,**I**) Expression of DCC intracellular P2–3 domain blocked netrin-1 attraction of chick spinal commissural axons. Axons expressing Venus YFP and DCC P2-3 domain were not attracted by the aggregates of HEK293 cells secreting netrin-1 (quantification in Fig. 6L, group I). Scale bar: 10 µm (F); 100 µm (I).

Movie 1. Live imaging of EB3-GFP comets in an E13 dorsal spinal cord neuron.

Movie 2. Live imaging of EB3-GFP comets in an E13 dorsal spinal cord neuron after netrin-1 stimulation.

Movie 3. Live imaging of EB3-GFP comets in an E13 dorsal spinal cord neuron transfected with TUBB3 shRNA in the absence of netrin-1.

Movie 4. Live imaging of EB3-GFP comets in an E13 dorsal spinal cord neuron transfected with TUBB3 shRNA in the presence of netrin-1.